Asymptotic Performance of ZF and MMSE Crosstalk Cancelers for DSL Systems

S. M. Zafaruddin*, Itsik Bergel, Amir Leshem

Faculty of Engineering, Bar-Ilan University, Ramat Gan 52900, Israel

Abstract

We present asymptotic expressions for user throughput in a multi-user digital subscriber line system (DSL) with a linear decoder, in increasingly large system sizes. This analysis can be seen as a generalization of results obtained for wireless communication. The features of the diagonal elements of the wireline DSL channel matrices make wireless asymptotic analyses inapplicable for wireline systems. Further, direct application of results from random matrix theory (RMT) yields a trivial lower bound. This paper presents a novel approach to asymptotic analysis, where an alternative sequence of systems is constructed that includes the system of interest in order to approximate the spectral efficiency of the linear zero-forcing (ZF) and minimum mean squared error (MMSE) crosstalk cancelers. Using works in the field of large dimensional random matrices, we show that the user rate in this sequence converges to a non-zero rate. The approximation of the user rate for both the

*Corresponding author

Email addresses: smzafar@biu.ac.il (S. M. Zafaruddin*), itsik.bergel@biu.ac.il (Itsik Bergel), leshema@biu.ac.il (Amir Leshem)

[1]Currently, S.M. Zafaruddin is with the department of Electrical and Electronics Engineering, BITS Pilani, Rajasthan-333031, India.

[2]A portion of this paper was presented at the IEEE ICSEE 2016 [1].

ZF and MMSE cancelers are very simple to evaluate and does not need to take specific channel realizations into account. The analysis reveals the intricate behavior of the throughput as a function of the transmission power and the channel crosstalk. This unique behavior has not been observed for linear decoders in other systems. The approximation presented here is much more useful for the next generation G.fast wireline system than earlier DSL systems as previously computed performance bounds, which are strictly larger than zero only at low frequencies. We also provide a numerical performance analysis over measured and simulated DSL channels which show that the approximation is accurate even for relatively low dimensional systems and is useful for many scenarios in practical DSL systems.
Keywords: Asymptotic Analysis, Digital Subscriber Lines, G. fast, Linear Processing,, MMSE, Random Matrix Theory, Wireline Channels, Zero Forcing.

---

1. Introduction

Wireline digital subscriber line (DSL) systems use the existing infrastructure of telephone networks to provide broadband services to customers [2]. The new G.fast standard targets fiber-like speed (e.g., upto 1 Gbps) over short copper loops [3], [4], [5]. Until the final migration of all copper lines to fiber in access networks, DSL technology is likely to continue to be used widely, and play a key role in the convergence of next generation wired and wireless technologies. Another wireline technology is the 10GBASE-T Ethernet to provide a data rate of 10 Gb/s over structured copper cabling systems. However, the performance of wireline systems is limited by inter-

ference caused by the electromagnetic coupling of transmissions from other wire pairs. Specifically, the main issue is far-end crosstalk (FEXT), which is generated by the transmitters at the opposite side of the binder [2].

With the advent of vectoring technology [6], [7], various techniques have been developed to cancel crosstalk in multichannel wireline systems [5]. These include linear zero-forcing (ZF) [8], [9] and linear minimum mean squared error (MMSE) equalizers [10], [11], and non-linear based techniques such as the ZF generalized decision feedback equalizer (ZF-GDFE) [12] and MMSE-GDFE [13]. Cendrillon *et al.* [8] [9] showed that the ZF processing is close to optimal in typical DSL channels due to the diagonal dominance of the channel matrix. Thus, over the years, the ZF method has become very popular for upstream decoding (e.g., [12]-[15]), and downstream precoding (e.g., [16]-[21]) in DSL systems. However, with increasing frequency, diagonal dominance declines and the MMSE canceler outperforms the ZF canceler particularly at higher frequency tones. While more advanced non-linear receivers have been proposed [6], [12], these simple receivers tend to be preferred, particularly in the computationally intensive crosstalk cancellation of DSL systems. The G.fast standard recommends the use of linear structures for crosstalk cancellation for 106 MHz [3].

The performance of the ZF canceler had been shown to be dependent on the diagonal dominance characteristics of the DSL channel [8, 9, 14, 15]. Newer performance bounds [14, 15] were shown to be even tighter, and guaranteed the ZF near optimally for even higher frequencies. The bounds in [15] are much simpler to evaluate, and better show the near optimality of ZF processing when the channel matrix is diagonally dominant. However,

with the increased bandwidth of G.fast, the FEXT is higher and all of these bounds in [8, 9, 14, 15] become irrelevant (they degenerate to a lower bound of 0). Surprisingly, in many cases the ZF canceler still performs well, and in other cases the MMSE canceler is close to optimal. However, no analysis has been conducted to confirm these outcomes.

In this work, we examine the asymptotic behavior of ZF and MMSE decoders for wireline channels as the number of jointly decoded users grows, using tools from the field of large dimensional random matrix theory (RMT). Most works on RMT have dealt with the case of zero-mean random matrices, and have investigated the asymptote of the spectrum of $N \times N$ random matrices $\mathbf{Z}_n\mathbf{Z}_n^H$ where $\mathbf{Z}_n$ has zero mean entries. For example, Marchenko and Pastur [22] and Silverstein and Bai [23] analyzed these matrices with i.i.d. entries, whereas Girko [24] and Khorunzhy et al. [25] discussed these matrices with non-i.i.d. entries. The case of non-zero mean random matrices has been less widely explored. Nevertheless, Dozier and Silverstein [26] and Hachem et al. [27] presented a deterministic equivalent of the empirical Stieltjes transform of $\mathbf{Z}_n\mathbf{Z}_n^H$, where $\mathbf{Z}_n = \mathbf{Y}_n + \mathbf{A}_n$ with $\mathbf{Y}_n$ as a zero mean random matrix and $\mathbf{A}_n$ as a sequence of deterministic matrices.

The use of large RMT enables a deterministic analysis of the performance of systems that are by nature random and quite complex. This approach has been applied to analyze the performance of linear decoders for wireless networks [28, 29, 30, 31, 32]. In particular, Liang et al. [30] used the results of [24] for asymptotic analysis of the MMSE performance in MIMO wireless systems whose channel coefficients are all identically distributed. However, the wireline system differs from the wireless system, and thus analysis meth-

ods for MIMO MMSE/ZF can not be readily applied in the wireline context. This is primarily because the diagonal elements in the wireline channel matrix are different from the non-diagonal elements, which is not the case in wireless systems. Thus, a novel approach is required to get useful results in wireline systems.

In this paper, we take a novel approach to the asymptotic analysis of large systems where we construct an alternative sequence of systems that includes the system of interest. We then use the results in [27] to derive an approximation of the spectral efficiency of linear ZF and MMSE decoders for wireline systems. We also provide numerical results over measured and simulated DSL channel matrices to demonstrate the accuracy of the analysis for various system parameters.

The presented approximation is very simple to evaluate and does not require the knowledge of the specific channel. As we approach the massive deployment stage of G.fast systems, there is a need to predict the achievable performance in various deployment scenarios. Analysis by simulation may help, but this will give the performance for a single setup for each run. Thus the presented analytical result is of a great value, as it can give the performance (at least approximate) for various setups. For example, SNR is used to effectively load bits on each tone for each user to improve the data rate performance. The performance of the ZF decoder is shown to decrease linearly with FEXT power up to the point where the FEXT power is equal to the direct channel power. If the FEXT power is larger than the direct channel power, the asymptotic performance of the ZF decoder approaches zero.

The MMSE decoder exhibits a more intricate behavior. For example, the asymptotic behavior of the output SNR as a function of the transmitted power p can have three different behaviors: it can be proportional to p, proportional to the square root of the p, or proportional to $p^{2/3}$ depending on the average FEXT power. The behavior of the MMSE SNR as a function of the FEXT power is also non-trivial. The output SNR can be either monotonically increasing with respect to the average FEXT power or can have a local minimum at a average FEXT power less than twice the gain of the direct channel, depending on the transmitted power, p. This intricate behavior is very different than the performance of MMSE decoders for any other scenario.

Note that the proposed approximation is much more optimistic than existing deterministic analyses [8], [12], [15] which placed limits on the sum of the absolute values of the FEXT terms.

We also show that the proposed asymptotic analysis degenerates into the wireless solution [30], with the proper choice of system parameters when the variables are indeed i.i.d. Thus, the analysis can be seen as a generalization of the [30] to a more general setup that includes the wireline scenario.

The rest of this paper is organized as follows. Section II defines the wireline system and channel models for DSL system. The novel asymptotic analysis approach is described in Section III. The performance of ZF and MMSE cancelers is described Section IV. Section V provides the performance evaluation using numerical analysis on measured and simulated channel data of DSL systems. Section VI concludes the paper.

2. System Model

2.1. System Setup

The multi-user wireline channel is modeled as a multiple-input multiple-output (MIMO) system (known as vectored system in DSL technology) with M users that are connected to the distribution point (DP) through a cable of M twisted pairs [5]. We consider upstream transmission and assume perfect synchronization among users. Discrete multi-tone (DMT) modulation is used that facilitates independent processing at each tone. The signal vector $\mathbf{y} \in \mathbb{C}^M$ received by the DP at any given symbol time and any given frequency tone can be written as:

$$\mathbf{y} = \sqrt{p}\mathbf{H}_{\mathrm{c}}\mathbf{x} + \mathbf{v}, \tag{1}$$

where p is the transmitted power at the given frequency tone, $\mathbf{H}_{\mathrm{c}} \in \mathbb{C}^{M\times M}$ is the channel matrix in which the i, j element represents the channel coefficient from user j to the ports of the i-th pair in the DP, $\mathbf{x} \in \mathbb{C}^M$ is a vector that contains the transmitted symbols of all users, $\mathbf{v} \in \mathbb{C}^M$ is a complex Gaussian noise vector distributed as $\mathcal{CN}(0, \sigma_v^2 I_M)$, where σ_v^2 denotes the variance of the noise components and I_M denotes the $M \times M$ identity matrix. We assume that all transmitted symbols (i.e., the elements of the vector $\mathbf{x}$) are independent and identically distributed (i.i.d.) random variables with zero mean and unit variance, and that the transmission powers of all users are equal.

2.2. DSL Channel Matrix $\mathbf{H}_{\mathrm{c}}$

The diagonal elements of the channel matrix $\mathbf{H}_{\mathrm{c}}$ represents the attenuation of the direct signals while the off-diagonal elements reflect the crosstalk.

The performance of a DSL system depends on this matrix of channel gains, which can be measured for a specific binder under specific environmental conditions. It is known that the diagonal part of a DSL channel is a function of frequency, loop length and physical parameters of the twisted pairs [2]. However, the variation of the gain of these direct channels between different wires with the same parameters is relatively small such that this direct channel gain is often considered to be deterministic. However, the off-diagonal elements depend on various other factors such as capacitance and the inductive imbalance between the pairs, non-uniform twisting, geometric imperfections of twisted pairs. These lead to relatively large variations in the crosstalk couplings. Hence, non-diagonal elements of the DSL channel matrix are often considered to be random [33, 34, 35, 36].

To analyze the performance of wireline systems, we need to know its channel matrix. However, such measurements are rarely available in advance and do not cover a wide range of scenarios. As a substitute, one can turn to statistical analysis. Statistical models are available and have been presented by Karipidis et al. [37] and Sorbara et al. [38] [36] for DSL systems. These models have been adopted by various studies of DSL systems (e.g., [14], [39], [40]).

A widely acceptable statistical model of the DSL FEXT coupling [38] $[H_c]_{ij}$, $i \neq j$ is given by

$$[H_c]_{ij} = K_{\text{fext}}[H_c]_{jj} f \sqrt{l_{ij}} C_{ij}, \forall i \neq j, \tag{2}$$

where f is frequency of operation, l_{ij} is coupling length, and K_{fext} is a constant that depends on the type of cable (e.g. for 24 AWG cables $K_{\text{fext}} = 1.59 \times 10^{-10}$). The term $[H_c]_{ij}$ denotes the direct path of the disturber. The

dispersion (excluding the phase) is modeled by a log-normal random variable, $C_{ij} = 10^{-0.05\chi(f)} \exp(j\phi)$ where $\chi(f)$ is a Gaussian random variable in dB with mean $\mu_{\text{dB}} = 2.33\,\sigma_{\text{dB}}$ and variance σ_{dB}, and ϕ is uniform phase in the interval $[0, 2\pi]$. The model of the direct path is given as:

$$[H_c]_{jj} = \exp(-lr), \tag{3}$$

where l is line length of the j-th user and r is the attenuation constant of the cable. Extensive measurement are used to derive these parametric cable models for diagonal and non-diagonal elements of the channel matrix. As seen in (2) and (3), the non-diagonal and diagonal elements are distributed differently.

Since the randomness of the DSL channel is exhibited in the non-diagonal elements and not in the diagonal part, we define a normalized FEXT matrix $\mathbf{Q}$ whose elements are

$$q_{ij} = \begin{cases} \frac{[H_c]_{ij}}{[H_c]_{jj}}, \forall i \neq j \\ 0, \forall i = j. \end{cases} \tag{4}$$

Thus, the channel matrix can be decomposed as:

$$\mathbf{H} = \mathbf{I} + \mathbf{Q}, \quad \mathbf{H}_{\text{c}} = \mathbf{HD}, \tag{5}$$

where $\mathbf{D} \in \mathbb{C}^{M \times M}$ is a diagonal matrix with the diagonal elements of $\mathbf{H}_c$ (thus, $\mathbf{H} \in \mathbb{C}^{M \times M}$ is the normalized channel matrix, in which all diagonal elements are equal to 1).

Our asymptotic performance analysis does not rely on the specifics of a particular model, and requires only the channel structure of (5) and the following assumption:

AS 1. *All (off-diagonal) elements of* $\mathbf{Q}$ *are identically distributed and statistically independent (i.i.d.).*

An examination of the parametric models in (2) and (3) shows the elements of $\mathbf{Q}$ are i.i.d in the case of an equal length binder. Note that these assumptions are less restrictive, and can also accommodate other channel models. In [1], we studied the statistical characterization of a DSL channel and verified these assumptions using measured data.

3. Asymptotic Analysis

3.1. Bounds on the Average Spectral Efficiency

In this sub-section, we evaluate the average spectral efficiency for the ZF and MMSE cancelers and derive a convenient lower bound. This analysis will be used to derive the asymptotic analysis in the next sub-section.

In order to extract the transmitted signals, the receiver multiplies the received signal by a linear equalizer (LE) matrix $\mathbf{F}$ so that the estimate of the vector $\mathbf{x}$ is:

$$\hat{\mathbf{x}} = \mathbf{F}\mathbf{y}. \tag{6}$$

The resulting signal to interference plus noise ratio (SINR) for the i-th user is:

$$\rho_i^{LE} = \frac{p\left|\left[\mathbf{F}\mathbf{H}_c\right]_{i,i}\right|^2}{p\sum_{j\neq i}\left|\left[\mathbf{F}\mathbf{H}_c\right]_{i,j}\right|^2 + \sigma_v^2\left[\mathbf{F}\mathbf{F}^H\right]_{i,i}}. \tag{7}$$

In the following, we denote the user spectral efficiency (i.e., throughput per unit bandwidth) for a given SINR over the considered frequency tone by $R_{\text{mod}}(\text{SINR})$. Using information theory arguments, we know that the achievable rate per unit bandwidth with an optimal coding modulation and receiver

is $R_{\text{mod}}(\text{SINR}) = \log_2(1 + \text{SINR})$. However, this rate, which utilizes quadrature amplitude modulation (QAM) constellations and finite block codes, is not achievable. Thus, all derivations in this work will apply to the general throughput measure $R_{\text{mod}}(\text{SINR})$ with the only condition that this function is a concave function.

In the numerical section (Section 5), where we need a specific throughput measure, we will adopt [41] $R_{\text{mod}}(\text{SINR}) = \log_2(1 + \text{SINR}/\Gamma)$, where Γ is termed as the SNR gap (or Shannon gap) and captures all system imperfections. Hence, for the SINR given in (7), the spectral efficiency for the i-th user is given by:

$$R_i^{\text{LE}} = R_{\text{mod}}\left(\rho_i^{\text{LE}}\right). \tag{8}$$

For reference we also define the single wire (SW) performance, if only one user transmits and the DP only uses the active wire for detection. The single wire rate is:

$$R_i^{\text{SW}} = R_{\text{mod}}\left(\eta_i\right), \tag{9}$$

where $\eta_i = \frac{p|d_{i,i}|^2}{\sigma_v^2}$ is the SW-SNR of the i-th user, and $d_{i,i}$ is the i-th element on the diagonal of matrix $\mathbf{D}$.

3.1.1. ZF Linear Canceler

For the ZF, the equalizer matrix is given as $\mathbf{F}^{\text{ZF}} = \mathbf{H}^{-1} = \mathbf{D}\mathbf{H}_{\text{c}}^{-1}$ which converts (6) to $\hat{\mathbf{x}} = \sqrt{p}\mathbf{D}\mathbf{x} + \mathbf{H}^{-1}\mathbf{v}$. The SINR of user i given the channel matrix, $\mathbf{H}_{\text{c}}$ is given by:

$$\rho_i^{\text{ZF}} = \frac{p\mathbb{E}\left[\left|d_{i,i}x_i\right|^2 \middle| d_{i,i}\right]}{\mathbb{E}\left[\left|\left[\mathbf{H}^{-1}\mathbf{v}\right]_i\right|^2 \middle| \mathbf{H}\right]} = \frac{\eta_i}{\left[\left(\mathbf{H}^H\mathbf{H}\right)^{-1}\right]_{i,i}}. \tag{10}$$

Thus, the average spectral efficiency of user i is given by:

$$R_i^{\mathrm{ZF}} = \mathbb{E}\left[R_{\mathrm{mod}}\left(\frac{\eta_i}{\left[(\mathbf{H}^H\mathbf{H})^{-1}\right]_{i,i}}\right)\right], \tag{11}$$

where the expectation is taken with respect to the distribution of the channel matrix. By comparing (9) to (11), we define the SNR loss with the ZF canceler as $\gamma_i^{\mathrm{ZF}} = \left[\left(\mathbf{H}^H\mathbf{H}\right)^{-1}\right]_{i,i}$ such that the spectral efficiency becomes:

$$R_i^{\mathrm{ZF}} = \mathbb{E}\left[R_{\mathrm{mod}}\left(\frac{\eta_i}{\gamma_i^{\mathrm{ZF}}}\right)\right]. \tag{12}$$

Using Jensen's inequality, the spectral efficiency is lower bounded by:

$$R_i^{\mathrm{ZF}} \geq \tilde{R_i}^{\mathrm{ZF}} = R_{\mathrm{mod}}\left(\frac{\eta_i}{\mathbb{E}[\gamma_i^{\mathrm{ZF}}]}\right). \tag{13}$$

Using assumption AS1, the distribution of γ_i^{ZF} is identical for all users. Hence

$$\mathbb{E}[\gamma_i^{\mathrm{ZF}}] = \frac{1}{M}\sum_{i=1}^{M}\mathbb{E}[\gamma_i^{\mathrm{ZF}}] = \mathbb{E}[\bar{\gamma}^{\mathrm{ZF}}], \tag{14}$$

where

$$\begin{aligned}\bar{\gamma}^{\mathrm{ZF}} &= \frac{1}{M}\sum_{j=1}^{M}\gamma_j^{\mathrm{ZF}} = \frac{1}{M}\sum_{i=1}^{M}\left[\left(\mathbf{H}^H\mathbf{H}\right)^{-1}\right]_{i,i} \\ &= \frac{1}{M}\mathrm{tr}\left[\left(\mathbf{H}^H\mathbf{H}\right)^{-1}\right].\end{aligned} \tag{15}$$

where $\mathrm{tr}[\cdot]$ denotes the trace of a matrix.

The substitution of (14) into (13) significantly simplifies the bound, and also allows us to apply asymptotic results.

3.1.2. MMSE Linear Canceler

For the MMSE, the canceler matrix can be obtained using $\text{argmin}_{\mathbf{F}}\, \mathbb{E}\left[||\sqrt{p}\mathbf{D}\mathbf{x} - \mathbf{F}\mathbf{y}||_2^2\right]$ to get[3]:

$$\mathbf{F}^{\text{MMSE}} = p|\mathbf{D}|^2\mathbf{H}^H(p\mathbf{H}|\mathbf{D}|^2\mathbf{H}^H + \sigma_v^2\mathbf{I})^{-1}, \tag{16}$$

where $|\mathbf{D}|^2$ is the square of absolute values of the elements of matrix $\mathbf{D}$. The error covariance matrix for the estimation of $\mathbf{x}$ is:

$$\begin{aligned}\mathbf{C}_e &= \mathbb{E}\left[(\sqrt{p}\mathbf{D}\mathbf{x} - \mathbf{F}\mathbf{y})\,(\sqrt{p}\mathbf{D}\mathbf{x} - \mathbf{F}\mathbf{y})^H\right] \\ &= p|\mathbf{D}|^2 - p|\mathbf{D}|^2\mathbf{H}^H(p\mathbf{H}|\mathbf{D}|^2\mathbf{H}^H + \sigma_v^2\mathbf{I})^{-1}p\mathbf{H}|\mathbf{D}|^2 \\ &= \sigma_v^2\left[\mathbf{H}^H\mathbf{H} + \frac{\sigma_v^2}{p}|\mathbf{D}|^{-2}\right]^{-1},\end{aligned} \tag{17}$$

where we used the matrix inversion lemma: $(\mathbf{A}+\mathbf{B}\mathbf{C})^{-1} = \mathbf{A}^{-1} - \mathbf{A}^{-1}\mathbf{B}(\mathbf{I}+\mathbf{C}\mathbf{A}^{-1}\mathbf{B})^{-1}\mathbf{C}\mathbf{A}^{-1}$. Manipulating (16) and (17) leads to the well known result:

$$\rho_i^{\text{MMSE}} = \frac{p\left[|\mathbf{D}|^2\right]_{ii}}{[\mathbf{C}_e]_{ii}} - 1. \tag{18}$$

Thus average spectral efficiency is:

$$R_i^{\text{MMSE}} = \mathbb{E}\left[R_{\text{mod}}\left(\frac{\frac{p}{\sigma_v^2}\left[|\mathbf{D}|^2\right]_{ii}}{\gamma_i^{\text{MMSE}}}\right)\right], \tag{19}$$

where $\gamma_i^{\text{MMSE}} = \left[\mathbf{H}^H\mathbf{H} + \frac{\sigma_v^2}{p}|\mathbf{D}|^{-2}\right]_{ii}^{-1}$. As the diagonal matrix $\mathbf{D}$ is deterministic, we can apply Jensen's inequality again as in the ZF case to bound (19) by:

$$R_i^{\text{MMSE}} \geq R_{\text{mod}}\left(\frac{\frac{p}{\sigma_v^2}\left[|\mathbf{D}|^2\right]_{ii}}{\bar{\gamma}}\right). \tag{20}$$

[3]Note that the multiplication on the left by $p|\mathbf{D}|^2$ is not required in a detection setup since it has no effect on the detection of the SINR.

where $\bar{\gamma}^{\text{MMSE}} = \frac{1}{M}\sum_{j=1}^{M}\gamma_j^{\text{MMSE}}$. Note that in the MMSE canceler case, the average SNR loss, i.e., the ratio between SW-SNR and the SNR at output of the MMSE canceler is given by:$\frac{\eta_i\bar{\gamma}}{\eta_i-\bar{\gamma}}$. Using matrix notation, the $\bar{\gamma}$-parameter of the MMSE canceler can be simplified:

$$\bar{\gamma}^{\text{MMSE}} = \frac{1}{M}\text{tr}\left[\left(\mathbf{H}^H\mathbf{H} + \frac{\sigma_v^2}{p}\left|\mathbf{D}\right|^{-2}\right)^{-1}\right]. \tag{21}$$

In the case that all diagonal elements of $\mathbf{D}$ are equal i.e., $d_{ii} = d \ \ \forall i$ such that $\mathbf{D} = d\mathbf{I}$ and using $\eta = \frac{|d|^2 p}{\sigma_v^2}$ in (21), we get

$$\bar{\gamma}^{\text{MMSE}} = \frac{1}{M}\text{tr}\left[\left(\mathbf{H}^H\mathbf{H} + \frac{1}{\eta}\mathbf{I}_M\right)^{-1}\right]. \tag{22}$$

In deriving (22) in the desired form, we have assumed that all the diagonal elements and transmit powers for each user are equal. Nevertheless, the asymptotic performance derived in (22) can also be applied if the diagonal elements and/or transmit powers are not equal but with small variance (naturally, with a higher approximation error). However, observing (10), it can be seen that the ZF asymptotic analysis can accommodate the unequal transmit powers.

Observing (15) and (22), it can be seen that performance metrics for both ZF and MMSE cancelers can be represented as:

$$\bar{\gamma} = \frac{1}{M}\text{tr}\left[\left(\mathbf{H}^H\mathbf{H} + \frac{1}{\xi}\mathbf{I}_M\right)^{-1}\right], \tag{23}$$

where for the MMSE $\xi = \eta$ and for the ZF $\xi \to \infty$. Representation of the performance metrics in the form of (23) allows us to apply the large matrix result of Hachem et al. [27].

In this work, we perform an asymptotic analysis of the $\bar{\gamma}$-parameter, and derive simple expressions that do not require the knowledge of the specific channel realizations. We show that in the asymptotic regime the performance of the ZF and MMSE cancelers converges to a constant and their average spectral efficiencies in (11) and (19) become tight.

3.2. Novel Asymptotic Analysis Approach

In this section, we derive an approximation to the $\bar{\gamma}$-parameter for both the ZF and MMSE cancelers using the method of large matrix analysis. Before we start the asymptotic analysis, we need to note that the traditional analysis approach as the system size grows to infinity ($M \to \infty$) does not lead to useful limits. In the ZF case, such an asymptotic analysis converges to a zero rate, which cannot give a reasonable approximation for the performance. In the MMSE case, the rate converges to a non-zero limit, but in a way that cannot account for the importance of the direct channel elements (the diagonal elements in the channel matrix). Instead, we present a novel approach in which we construct a new sequence of systems such that the system of interest (described in the previous section) is an element in the sequence, and the rate of each user in this sequence of systems converges to a non-zero limit.

To derive this new sequence of systems, we define:

$$\mathbf{\Sigma}_n = \mathbf{I}_n + \sqrt{\frac{M-1}{n-1}}\mathbf{Q}_n, \tag{24}$$

a sequence of matrices with increasing sizes, where $n \geq 2$ and $\mathbf{Q}_n$ is an $n \times n$ random matrix with zero diagonal and i.i.d. elements outside the diagonal. We set the distribution of each non-diagonal element of $\mathbf{Q}_n$ ($q_{n,i,j}$

for $i \neq j$) to be identical to the distribution of a non-diagonal element in $\mathbf{Q}$, and require that $\mathbb{E}\left[|q_{1,2}|^{4+\epsilon}\right]$ be bounded for some $\epsilon > 0$. Note that $\mathbf{\Sigma}_n$ has the same distribution as $\mathbf{H}$. Thus, the definition of $\mathbf{\Sigma}_n$ establishes the sequence of arbitrary matrices which intersect with our system model when $n = M$. More specifically, this sequence is constructed such that the total FEXT power per user is constant for all system sizes.

This novel asymptotic analysis approach is illustrated in Fig. 1, which depicts $\bar{\gamma}$ in (23) with $\xi \to \infty$ (i.e., for the ZF system). The blue squares show that the parameter $\bar{\gamma}$ with original channel matrix $\mathbf{H}$ diverges as the system size, M, grows to infinity (and hence the rate converges to zero). On the other hand, the alternative sequence of (24) (depicted by circles) converges to a finite bound (as shown by the dashed line). The original and the alternative sequences intersect at the size of interest $n = M = 200$. Clearly in this scenario the asymptotic limit (as depicted by the dashed red line) gives a good approximation of the parameter $\bar{\gamma}$ for both sequences. Note that Fig. 1 illustrates the asymptotic analysis approach using a simple random channel. Extensive numerical analysis for DSL channels is presented in Section 5.

Using (23), the associated $\bar{\gamma}$-parameter for the alternative sequence system of size n is represented as

$$\tilde{\gamma}_n = \frac{1}{n}\mathrm{tr}\left[\left(\mathbf{\Sigma}_n^H \mathbf{\Sigma}_n + \frac{1}{\xi}\mathbf{I}\right)^{-1}\right]. \tag{25}$$

These two new quantities, $\mathbf{\Sigma}_n$ and $\tilde{\gamma}_n$, will be used in the following to conduct the asymptotic analysis as $n \to \infty$. The asymptotic analysis results in a deterministic equivalent for both ZF and MMSE cancelers, which describes the behavior of the lower bound as the system size becomes large enough.

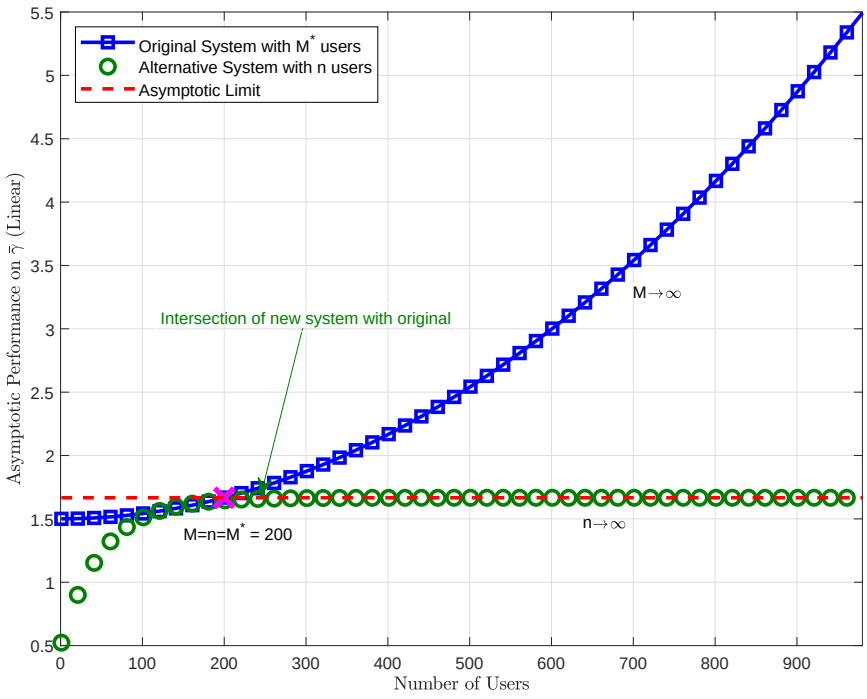

Figure 1: An example of the construction of the sequence of systems for asymptotic analysis.

It is important to note that practically speaking, our approach has exactly the same meaning as any other asymptotic analysis. That is, if the system of interest is far enough along in the sequence, its performance is well approximated by the asymptotic results. Also note that in most types of asymptotic analysis, the important question: "How close is the system of interest to the asymptotic result?" is primarily dealt with through simulations (for example in large matrix analysis [42]–[44], and in asymptotic SNR analyses using 'degrees of freedom' [45]–[47]). This question will be addressed below by an analysis using some special cases and extensively through numerical and

simulation examples in Section 5.

For the asymptotic analysis, we use the theorem presented in Hachem et al. for non-centralized large random matrices [27]. To use the result, we adapt our parameters to the parameters in [27] by setting $\sigma_{i,j}^2(n) = \frac{n}{n-1}(M-1)\mathbb{E}\left[|q_{n,i,j}|^2\right]$, and $x_{i,j} = \frac{q_{n,i,j}}{\sqrt{\mathbb{E}\left[|q_{n,i,j}|^2\right]|_{i\neq j}}}$. Hence, the theorem presented in Hachem et al. [27] can be represented in the following Theorem for our system setup.

Theorem (Hachem et al. [27])**.** *Consider an $n\times n$ random matrix $\mathbf{Y}$ in which the i,j entry is given by $y_{i,j} = \frac{\sigma_{i,j}(n)}{\sqrt{n}}x_{i,j}$, and $x_{i,j}$ are i.i.d. random variables with zero mean and unit variance, which satisfy the following assumptions:*

(1) There exists an $\varepsilon > 0$ such that: $\mathbb{E}\left[|x_{i,j}|^{4+\epsilon}\right] < \infty$

(2) There exists a finite number σ_{max} such that: $\sup_{n\geq 1}\max_{i,j}|\sigma_{i,j}(n)| \leq \sigma_{max}$

Let $\mathbf{\Sigma} = \mathbf{I} + \mathbf{Y}$. There exists a deterministic $n\times n$ matrix-valued function $\mathbf{T}(z)$ analytic in $\mathbb{C}-\mathbb{R}^+$ such that, almost surely:

$$\lim_{n\to\infty}\left(\frac{1}{n}\mathrm{tr}\left[\left(\mathbf{\Sigma}\mathbf{\Sigma}^H - z\mathbf{I}_n\right)^{-1}\right] - \frac{1}{n}\mathrm{tr}\left[\mathbf{T}(z)\right]\right) = 0 \tag{26}$$

and $\mathbf{T}(z)$ is the unique positive solution of:

$$\begin{aligned}\mathbf{T}(z) &= \left(\mathbf{\Psi}^{-1}(z) - z\tilde{\mathbf{\Psi}}(z)\right)^{-1}\\ \tilde{\mathbf{T}}(z) &= \left(\tilde{\mathbf{\Psi}}^{-1}(z) - z\mathbf{\Psi}(z)\right)^{-1}\end{aligned} \tag{27}$$

$$\begin{aligned}\mathbf{\Psi}(z) &= \mathrm{diag}\left(\psi_1(z),\ldots,\psi_n(z)\right)\\ \tilde{\mathbf{\Psi}}(z) &= \mathrm{diag}\left(\tilde{\psi}_1(z),\ldots,\tilde{\psi}_n(z)\right)\end{aligned} \tag{28}$$

$$\begin{aligned}\psi_i(z) &= -z^{-1}\left(1+\mathrm{tr}\left(\tilde{\mathbf{\Omega}}_i\tilde{\mathbf{T}}(z)\right)/n\right)^{-1}\\ \tilde{\psi}_j(z) &= -z^{-1}\left(1+\mathrm{tr}\left(\mathbf{\Omega}_j\mathbf{T}(z)\right)/n\right)^{-1}\end{aligned} \tag{29}$$

$$\begin{aligned}\tilde{\mathbf{\Omega}}_i &= \text{diag}\left(\sigma_{i1}^2(n), \ldots, \sigma_{in}^2(n)\right) \\ \mathbf{\Omega}_j &= \text{diag}\left(\sigma_{1j}^2(n), \ldots, \sigma_{nj}^2(n)\right).\end{aligned} \tag{30}$$

The main rationale for using Theorem 1 is that the performance of linear cancelers can be represented as a deterministic function that does not depend on the actual channel realization. In addition, the solution in (26)-(30) only involves diagonal matrices in contrast to the matrix inversion required in the original problem. While the result of this theorem is still quite complicated, we will show that we can simplify the equations to a closed form performance expression.

As mentioned above, in this work we cannot directly apply the Hachem theorem to the problem at hand. Instead we use our alternative choice of $\mathbf{\Sigma}$ which enables accurate approximation of the parameters. In the next subsection, we derive our main theorem by applying the Hachem theorem to the new sequence of systems, defined in (24). We then further use the system properties to derive a simple expressions for our performance, characterized by γ^o.

3.3. Asymptotic Analysis Theorems

Theorem 1. *Let*

$$\sigma^2 = (M-1)\mathbb{E}\left[|q_{i,j}|^2\right]_{i \neq j} \tag{31}$$

be the total average FEXT power, then the deterministic equivalent γ° is the unique real and positive root of the cubic equation in t

$$\sigma^4 t^3 + 2\sigma^2 t^2 + (1 + \xi - \xi\sigma^2)t - \xi = 0. \tag{32}$$

As the system size grows to infinity, $\tilde{\gamma}_n$-parameter defined in (25) *will converge almost surely to the deterministic equivalent:*

$$\lim_{n\to\infty}(\gamma^{\circ}-\tilde{\gamma}_n)=0. \tag{33}$$

Proof. Comparing (26) with (25) and noting that the matrix $\mathbf{\Sigma}\mathbf{\Sigma}^H$ is full rank, asymptotic performance on the $\tilde{\gamma}_n$ for the asymptotic analysis can be obtained by evaluating (26):

$$\lim_{n\to\infty}\tilde{\gamma}_n=\gamma^{\circ}\triangleq\lim_{n\to\infty,}\frac{1}{n}\mathrm{tr}\left[\mathbf{T}\left(-\frac{1}{\xi}\right)\right]. \tag{34}$$

To evaluate (34), we simplify equations (26)-(30). Due to the homogeneity of the variance matrix, Σ_n (except for its diagonal), we have $\mathbf{\Omega}_i=\tilde{\mathbf{\Omega}}_i$ and the j-th element on the diagonal of $\mathbf{\Omega}_i$ equals $\frac{n}{n-1}\sigma^2$ if $j\neq i$ and 0 if $j=i$. Since $\mathbf{T}(-\frac{1}{\xi})$ is a diagonal matrix, we define $t_i=[\mathbf{T}(-\frac{1}{\xi})]_{i,i}$ and $t=(\mathrm{tr}[\mathbf{T}(-\frac{1}{\xi})])/n$, which yields:

$$\mathrm{tr}\left(\mathbf{\Omega}_j\mathbf{T}\left(-\frac{1}{\xi}\right)\right)=\frac{n}{n-1}\sigma^2(nt-t_i). \tag{35}$$

Using the same definitions for $\tilde{t}_i$ and $\tilde{t}$, equation (27) becomes:

$$\begin{aligned}t_i&=\frac{1}{\frac{1}{\xi}\left(1+\frac{\sigma^2}{n-1}(nt-t_i)\right)+\frac{1}{1+\frac{\sigma^2}{n-1}(\tilde{t}-\tilde{t}_i)}},\\ \tilde{t}_i&=\frac{1}{\frac{1}{\xi}\left(1+\frac{\sigma^2}{n-1}(\tilde{t}-\frac{\tilde{t}_i}{n})\right)+\frac{1}{1+\frac{\sigma^2}{n-1}(t-\frac{t_i}{n})}}.\end{aligned} \tag{36}$$

Due to the symmetry between all users, $i=1,\ldots,n$, in (36) and the uniqueness of the solution, we have $t_i=t$ and $\tilde{t}_i=\tilde{t}$ which simplifies to:

$$\begin{aligned}t&=\frac{1}{\frac{1}{\xi}\left(1+\sigma^2t\right)+\left(1+\sigma^2\tilde{t}\right)^{-1}},\\ \tilde{t}&=\frac{1}{\frac{1}{\xi}\left(1+\sigma^2\tilde{t}\right)+\left(1+\sigma^2t\right)^{-1}}.\end{aligned} \tag{37}$$

Furthermore, using the uniqueness again, the symmetry between t and $\tilde{t}$ gives $\tilde{t} = t$ and thus

$$t = \frac{1}{\frac{1}{\xi}(1+\sigma^2 t) + (1+\sigma^2 t)^{-1}}. \tag{38}$$

A simple manipulation on (38) yields the cubic equation in (32). Further, due to the uniqueness property of the theorem in Hachem et al. [27], the solution in (32) ensures a single unique root. This uniqueness property has been further investigated in Section IV (see Corollary 2). □

In the next section, we use Theorem 1 to characterize the performance of the ZF and MMSE interference cancelers. Before that, we briefly present a more general result that can help characterize performance in non-homogeneous networks. Assume that all the elements of matrix $\mathbf{Q}$ still have the same distribution, but can have a different variance. Define $\sigma_u^2 = (M-1)\max[|q_{i,j}|^2]\big|, \forall i,j, i \neq j$ and $\sigma_l^2 = (M-1)\min[|q_{i,j}|^2]\big|, \forall i,j, i \neq j$ as the maximum and the minimum variance of an element in the normalized FEXT matrix $\mathbf{Q}$, respectively. The following theorem provides a single parameter bounds on the $\tilde{\gamma}_n$.

Theorem 2. *If $\sigma_u^2 < 1$ and $\sigma_l^2 < \sigma_u^2$ are the maximum and minimum of the absolute squared values of the normalized FEXT, respectively and $t = \frac{1}{n}\mathrm{tr}[\mathbf{T}(-\frac{1}{\xi})]$, then*

$$\begin{aligned} \gamma^\circ &\leq \frac{1}{1-\sigma_u^2}, \\ \lim_{\xi\to\infty} \gamma^\circ &\geq \frac{1}{1-\sigma_l^2}. \end{aligned} \tag{39}$$

Proof. The proof is provided in Appendix A. □

Note that this theorem can also be used instead of Theorem 1 to characterize the performance of the ZF canceler in the homogeneous case ($\sigma_u^2 = \sigma_l^2$).

4. Performance of ZF and MMSE Cancelers

In this section, we use Theorem 1 to characterize the asymptotic performance of the MMSE and ZF cancelers.

4.1. Asymptotic Analysis of ZF Performance

Corollary 1 (Deterministic equivalent of the associated average SNR loss)**.** *Let*

$$\sigma^2 = (M-1)\mathbb{E}\left[|q_{i,j}|^2\right]_{i\neq j}. \tag{40}$$

be the total FEXT power and the deterministic equivalent SNR loss given, respectively. If $\sigma^2 < 1$, as the system size grows to infinity, the average SNR loss of ZF will converge almost surely to the deterministic equivalent SNR loss, γ^o:

$$\lim_{n\to\infty}(\gamma^\circ - \tilde{\gamma}_n) = 0, \tag{41}$$

where

$$\gamma^\circ = (1-\sigma^2)^{-1}. \tag{42}$$

If $\sigma^2 \geq 1$, then $\tilde{\gamma}_n$ is not bounded ($\lim_{n\to\infty}\tilde{\gamma}_n = \infty$), i.e., the user rate will go to zero.

Proof. Comparing (25) with (15) for the ZF, the deterministic equivalent of the SNR of the ZF canceler is given by by the root of (32) when $\xi \to \infty$ such that

$$\gamma^{\mathrm{ZF}} \triangleq \lim_{\xi\to\infty}\gamma^\circ. \tag{43}$$

If t is bounded, we use $\lim_{\xi\to\infty}$ in (32) to get

$$(1-\sigma^2)t - 1 = 0, \tag{44}$$

which leads to (42). However, if $t(z)$ is unbounded, we can rewrite equation (32) to get:

$$\sqrt{-\frac{1}{\xi}}t = \frac{1}{-\left(\sqrt{-\frac{1}{\xi}} + \sigma\sqrt{-\frac{1}{\xi}t}\right) + \left(\sqrt{-\frac{1}{\xi}} + \sigma\sqrt{-\frac{1}{\xi}t}\right)^{-1}}. \tag{45}$$

The unique solution of this equation when we take the limit as $\xi \to \infty$ is:

$$\lim_{\xi\to\infty} \sqrt{\frac{1}{\xi}}t = \frac{\sqrt{\sigma^2 - 1}}{\sigma^2}, \tag{46}$$

where a positive solution is obtained when $\sigma^2 \geq 1$. Hence, if $\sigma^2 > 1$, $\sqrt{t/\xi}$ converges to a finite bound, and t is not bounded. □

Thus, if M is large enough and $\sigma^2 < 1$, γ° is a good approximation for $\tilde{\gamma}_n$. In this case, our asymptotic analysis provides a good approximation for the rate in the original system of interest. Compared to (13), and assuming that the Jensen inequality is tight, we conclude that the user rates in the system using the ZF canceler are well approximated by:

$$R_i^{\mathrm{ZF}} \simeq R_{\mathrm{mod}}\left(\frac{\eta_i}{\gamma^\circ}\right), i = 1 \cdots M. \tag{47}$$

By inspecting (47), this approximation is only a function of the number of users, M, and the statistics of the channel FEXT. Thus, the result of Lemma 1 is very useful for system characterization, and can easily determine the regimes in which the ZF linear canceler is efficient and the regimes for which it is not a good choice.

As can be seen from (40), for any system setup, the approximation will hold up to a certain size M. This provides another illustration of the fact that (47) will be accurate for any finite M. Obviously, this does not contradict Theorem 1, which is derived as n (and not M) grows to infinity. Nevertheless,

we need to provide an alternative intuition that will predict when (47) is accurate. In Section 5 we present a numerical study of the accuracy of (47). We show that this approximation is very good for small values of σ^2, and holds well as long as $\sigma^2 < 0.5$.

The above Corollary 1 determines that asymptotic ZF performance is not useful when $\sigma^2 \geq 1$. However, as the ZF and MMSE are equivalent at high SNR, the MMSE asymptotic result can be used to approximate the ZF performance when $\sigma^2 \geq 1$ unlike the general performance bounds on these schemes where the ZF performance is used to predict MMSE performance.

4.2. Asymptotic Analysis of MMSE Performance

By comparing (25) and (22), the deterministic equivalent of γ to compute the SNR loss for the MMSE can be obtained directly from (32) by substituting $\xi = \eta$. However, for MMSE, it is more convenient to derive a direct approximation for the SNR, ρ as defined in (18).

Corollary 2 (Deterministic equivalent of the MMSE SNR)**.** *Let*

$$\sigma^2 = (M-1)\mathbb{E}\left[|q_{i,j}|^2\right]_{i\neq j}, \tag{48}$$

and η is the AWGN SNR, then the asymptotic SNR at the MMSE output is given by the positive root of

$$\rho^3 - S\rho^2 + Q\rho - P = 0, \tag{49}$$

where $S = \eta - \eta\sigma^2 - 2$, $Q = 1 - 2\eta$ and $P = \eta^2\sigma^4 + \eta\sigma^2 + \eta$. The asymptotic SNR is given by the positive root:

$$\begin{aligned}\rho^o = -\frac{1}{3}\Big(&- S + (-0.5 + 0.5\sqrt{3}i)^k\Delta + \\ &\frac{S^2 - 3Q}{(-0.5 + 0.5\sqrt{3}i)^k\Delta}\Big), k = 0, 1, 2\end{aligned} \tag{50}$$

where $\Delta = \sqrt[3]{\frac{9SQ-2S^3-27P-\sqrt{(9SQ-2S^3-27P)^2-4(S^2-3Q)^3}}{2}}$.

Proof. The cubic equation in (49) is obtained directly from (32) by substituting $\xi = \eta$ and $\rho = \eta/\gamma - 1$ (see (20)). The closed form solution in (50) can be obtained using Cardano's method.

To show that exactly one root of (49) is positive, we denote the three roots as ρ_1, ρ_2, and ρ_3. Note that these roots are either all real, or one root is real while the others form a complex conjugate pair. We observe that the three roots satisfy: $P = \rho_1\rho_2\rho_3$, $S = \rho_1 + \rho_2 + \rho_3$ and $Q = \rho_1\rho_2 + \rho_2\rho_3 + \rho_3\rho_1$. When P is positive the number of negative (real) roots is even. If there are 2 negative roots, the third is the only positive root and we are done. Thus, we need only consider the case where there are no negative roots; i.e., either all roots are positive roots, or we have 1 positive and 2 complex roots. More specifically, we just need to rule out the case of all positive roots. This an be done if we either show that $S < 0$ or that $Q < 0$. Finally $Q < 0$ if $\eta > 0.5$, while $\eta \leq 0.5$ guarantees that $S < 0$. Thus, in all cases at least one S and Q is negative, which rules out the possibility of all positive roots and completes the proof. □

Thus, if M is large enough, γ° is a good approximation for $\tilde{\gamma}_n$, and thus ρ° in (50) provides a good approximation of the MMSE SNR. As compared to (20), the user rates in the system are well approximated by:

$$R^{\text{MMSE}} \simeq R_{\text{mod}}\Big(\rho^\circ\Big). \tag{51}$$

Similar to the ZF, this approximation is only a function of the number of users, M, and the statistics of the channel FEXT. Thus, the result of Corollary 2 is very useful for system characterization, and can easily determine

the regimes in which linear cancelers are efficient and the regimes for which they are not a good choice. The asymptotic performance for the MMSE can be obtained for any average FEXT value σ^2, whereas the asymptotic rate of the ZF canceler is zero for $\sigma^2 \geq 1$.

The asymptotic SNR using the MMSE canceler exhibits interesting and complicated behavior as a function of the SW-SNR and the FEXT power. To provide additional insights, the following Corollary outlines the behavior of ρ° as a function of η and σ^2.

Corollary 3. *The behavior of the asymptotic SNR using the MMSE canceler as a function of η and σ^2 can be characterized by:*

(a) At low SW-SNR, η, the asymptotic SNR can be approximated by $\rho^\circ \approx (1+\sigma^2)\eta$.

(b) At high SW-SNR, η, the behavior of asymptotic SNR, depends on the total FEXT power:

- *If $\sigma^2 < 1$, then $\rho^\circ \approx (1-\sigma^2)\eta$.*
- *If $\sigma^2 = 1$, then $\rho^\circ \approx \sigma^4\eta^{2/3}$.*
- *If $\sigma^2 > 1$, then $\rho^\circ \approx \frac{\sigma^2}{\sqrt{\sigma^2-1}}\sqrt{\eta}$.*

(c) If σ^2 is very small, the SNR can be approximated by: $\rho^\circ = \eta + \eta\frac{1-\eta}{\eta+1}\sigma^2$.

(d) If $\eta \leq 1$, the SNR, ρ°, increases monotonically with σ^2.

(e) If $\eta > 1$ then:

- *The SNR has local minima with respect to σ^2.*

- *The location of the minima is at* $0 \leq \sigma^2 \leq 1$ *for* $1 < \eta < 2.7$*, at* $1 \leq \sigma^2 \leq 2$ *for large* η*, and asymptotically approach* $\sigma^2 = 2$ *as* $\eta \to \infty$.

(f) For large σ^2 *the SNR approaches* $\sqrt{\eta\sigma^2}$.

This corollary leads to several interesting observations about the behavior of the MMSE receiver. Below, we first discuss this behavior and then give the proof of the corollary.

Part (a) is quite trivial. At low SNR, the interference is negligible, and the only issue is the total energy received relative to the Gaussian noise.

Part (b) presents the unique behavior of the MMSE receiver in the asymptotic regime. In any finite system at a high enough SNR, the performance of the MMSE converges to the performance of the ZF receiver. This indeed happens for $\sigma^2 < 1$. But, for $\sigma^2 > 1$, the ZF performance converges to 0, while the MMSE is proportional to the square root of the SNR. The case of $\sigma^2 = 1$ lies on the border between the two other cases, but has a unique asymptotic behavior of its own.

It is interesting to note that unlike most results presented in this work, the convergence of the ZF performance to 0 at σ^2 typically happens at very large system size. Thus, it was not observed in most of results in our numerical section. On the other hand, the similarity between MMSE and ZF at high SNRs does hold even for quite large systems, and hence, for $\sigma^2 > 1$, we found that asymptotic MMSE performance gives a better prediction for the performance of ZF receivers at practical system sizes than asymptotic ZF performance.

Part (c) confirms that if σ^2 is low, the direct channel is dominant. In the extreme case of $\sigma^2 = 0$, the result $\rho^\circ = \eta$ is very intuitive, since the wireline channel matrix $\mathbf{H}_c$ becomes a diagonal and the MMSE-SNR converges to the SW-SNR.

Part (d) demonstrates (as in Part (a)) that for low SW-SNR the MMSE canceler can indeed use the FEXT, and the rate increases with σ^2 (although the low SNR regime is not practical in DSL).

Part (e) illustrates the most unique characteristic of MMSE performance as a function of the FEXT power (σ^2). The user SNR can either be monotonically decreasing, or have a single local minimum. In particular, in the high SNR which is more typical of most of wireline systems, the SNR will decrease for low FEXT powers but will eventually increase when the FEXT is large.

In Section 5, we present a numerical study of the accuracy of (49) and (51) for a general convergence analysis.

Proof. Although (50) gives a closed form expression for ρ°,in all the proofs we found it more convenient to start again with (49).

Part (a) is proved by substituting the low η approximations into (49): $S \approx -2$, $Q \approx 1$ and $P \approx \eta(1+\sigma^2)$, resulting in:

$$\rho^3 + 2\rho^2 + \rho \approx \eta(1+\sigma^2). \tag{52}$$

Realizing that ρ will also be very small, we can drop the higher powers of ρ, which leads directly to: $\rho \approx \eta(1+\sigma^2)$.

Part (b) is proved through the same approach, using the high η approxi-

mations: $S \approx \eta(1-\sigma^2)$, $Q \approx -2\eta$ and $P \approx \eta^2\sigma^4$, resulting in:

$$\rho^3 - \eta(1-\sigma^2)\rho^2 - 2\eta\rho - \eta^2\sigma^4 \approx 0. \tag{53}$$

Noting again that if η is large ρ will also be large, the third term will always be dominated by the other terms, and can be neglected:

$$\rho^3 - \eta(1-\sigma^2)\rho^2 - \eta^2\sigma^4 \approx 0. \tag{54}$$

Now, we need to distinguish between the three cases. When $\sigma^2 < 1$ the third term in (54) is negligible, leading directly to $\rho \approx \eta(1-\sigma^2)$. The proof for the second and third cases is equally simple, by noting that if $\sigma^2 = 1$, the second term in (54) vanishes, whereas if $\sigma^2 > 1$ the first term is negligible.

Part (c) is proved by first noting that for $\sigma^2 = 0$, the positive root of the cubic equation in (49) is (as expected) $\rho^\circ = \eta$. Next, we evaluate the partial derivative ρ° with respect to σ^2, through the implicit derivative of Equation (49):

$$\begin{aligned} \rho^{'\circ} = \frac{d\rho^\circ}{d(\sigma^2)} &= \frac{S'\rho^{2\circ} - Q'\rho^\circ + P'}{3\rho^{2\circ} - 2S\rho^\circ + Q} \\ &= \frac{-\eta\rho^{2\circ} + 2\eta^2\sigma^2 + \eta}{3\rho^{2\circ} - 2(\eta - \eta\sigma^2 - 2)\rho^\circ + 1 - 2\eta}. \end{aligned} \tag{55}$$

For $\sigma^2 = 0$, and also using $\rho^\circ = \eta$ in (55), we get

$$\rho^{'\circ} = \eta\frac{1-\eta}{\eta+1}. \tag{56}$$

Thus, part (c) of the Corollary is obtained as a first order Taylor approximation. Note that part (c) shows that if $\eta < 1$, the first-order approximated SNR, ρ°, increases monotonically with σ^2. However, part (d) illustrates more stringent conditions on the monotonicity of the asymptotic SNR.

Part (d) is proved by finding the extremal points of ρ° as a function of σ^2. Using $\rho'^{\circ} = 0$ in (55) gives:

$$\rho_*^2 = 2\eta\sigma_*^2 + 1, \tag{57}$$

where σ_*^2 ans ρ_* are the extremal point of the average FEXT and the SNR value at that point, respectively. We use (57) in (49) to get the extremal point of the asymptotic SNR:

$$\rho_* = \frac{\eta^2\sigma_*^2(2-\sigma_*^2) + 2\eta(1-2\sigma_*^2) - 2}{2\eta(\sigma_*^2 - 1) + 2}. \tag{58}$$

Recalling that the SNR must be positive, we check when (58) is positive. We note that the numerator is positive only for:

$$1 - \frac{2}{\eta} - \sqrt{1 - \frac{2}{\eta} + \frac{2}{\eta^2}} < \sigma_*^2 < 1 - \frac{2}{\eta} + \sqrt{1 - \frac{2}{\eta} + \frac{2}{\eta^2}}, \tag{59}$$

while the denominator is positive only for:

$$\sigma_*^2 > 1 - \frac{1}{\eta}. \tag{60}$$

By comparing the last two conditions, we conclude that $\rho_* > 0$ only for:

$$1 - \frac{1}{\eta} < \sigma_*^2 < 1 - \frac{2}{\eta} + \sqrt{1 - \frac{2}{\eta} + \frac{2}{\eta^2}}. \tag{61}$$

The proof of Part (d) is completed by noting that when $\eta < 1$ (61) cannot be satisfied; hence, there is no extremal point of ρ_*.

Part (e) is proved by noting that (61) can be satisfied when $\eta > 1$, and evaluating the range of σ^2 for specific values of η. The asymptotic behavior for large η is obtained by comparing the square root of (57) with (58), and taking the large η asymptotic:

$$\sqrt{2/\eta} = \frac{\sqrt{\sigma_*^2}(2-\sigma_*^2)}{2(\sigma_*^2 - 1)}. \tag{62}$$

As the left hand side goes to zero for large η, we must have $\sigma_*^2 \to 2$.

Part (f) is proved in Theorem 3, and discussed in the next subsection. $\square$

4.3. Comparison to wireless asymptotic results

One natural question is how the proposed analysis with assumptions AS1 and AS2 compares to the results for wireless channels [30]. In the wireless case, the SNR at the output of the MMSE receiver was shown to be (in terms of the parameters used in this paper):

$$\rho^{\circ}_{\text{wireless}} = -0.5 + 0.5\sqrt{1 + 4\eta\sigma^2}. \tag{63}$$

However, this was derived for a channel matrix in which all elements are i.i.d., as opposed to the wireline channel matrix, in which the diagonal terms are fixed. To enable a comparison, we need to consider the case in which the effect of the diagonal elements on the SNR is negligible. This happens if we take σ^2 to infinity, and η to zero while keeping their product constant (to maintain a finite output SNR). The following theorem proves that in this special case, the two solutions are identical. As such our solution can be seen as a generalization of [30] to include both wireline and wireless channels.

Theorem 3. *When $\sigma^2 \to \infty$ and $\eta \to 0$ such that $\eta\sigma^2$ remains constant (i.e., the wireline channel approaches the wireless channel), then $\rho^{\circ} \to -0.5 + 0.5\sqrt{1 + 4\eta\sigma^2} = \rho^{\circ}_{\text{wireless}}$ is the only positive root of (49).*

Proof. While we can work directly with the solution of (50), in this case, it is more convenient to go back to the cubic equation in (49). Using $\eta \to 0$ while $\eta\sigma^2$ is constant, equation (49) can be written as:

$$(\rho + 1)^3 + (\eta\sigma^2 - 1)(\rho + 1)^2 - 2\eta\sigma^2(\rho + 1) - \eta^2\sigma^4 = 0. \tag{64}$$

Using long division, it can be seen that $\rho^{\circ} = -0.5 + 0.5\sqrt{1+4\eta\sigma^2}$, which exactly equal to the $\rho^{\circ}_{\text{wireless}}$ in (63), is one of the three roots of (64). The other two roots are the solution of the quadratic equation:

$$\begin{aligned}(\rho+1)^2 + (-0.5 + \eta\sigma^2 + 0.5\sqrt{1+4\eta\sigma^2})(\rho+1) \\ +\eta\sigma^2(-0.5 + 0.5\sqrt{1+4\eta\sigma^2}) = 0.\end{aligned} \tag{65}$$

The solution of (65) yields the two roots: $\alpha = -1 - \rho^{\circ}$ and $\beta = -1 - \eta\sigma^2$. Since ρ^0, η and σ^2 are positive, the cubic equation (64) has a single positive root and two negative roots. □

Theorem 3 confirms that the wireless solution [30] is a special case of the generalized solution proposed in this paper. Thus the proposed asymptotic analysis performs better for wireline channels than the result developed for wireless channels [30] and is expected to converge excellently at lower values of SNR and σ^2. Hence, we expect that both solutions will yield similar results when the diagonal elements of the channel matrix are similar to the non-diagonal elements. However, the proposed asymptotic result should perform better for typical wireline channels where the diagonal elements are distributed independently to the non-diagonal elements.

5. Numerical and Simulation Analysis

In this section, we study the convergence of the actual SNR to the asymptotic analysis of linear cancelers for wireline systems through computer simulations based on MATLAB software. First, we consider synthetic wireline channel models, and then consider channel models from G.fast [3] and VDSL [48] wireline standards as an example to demonstrate the proposed analysis.

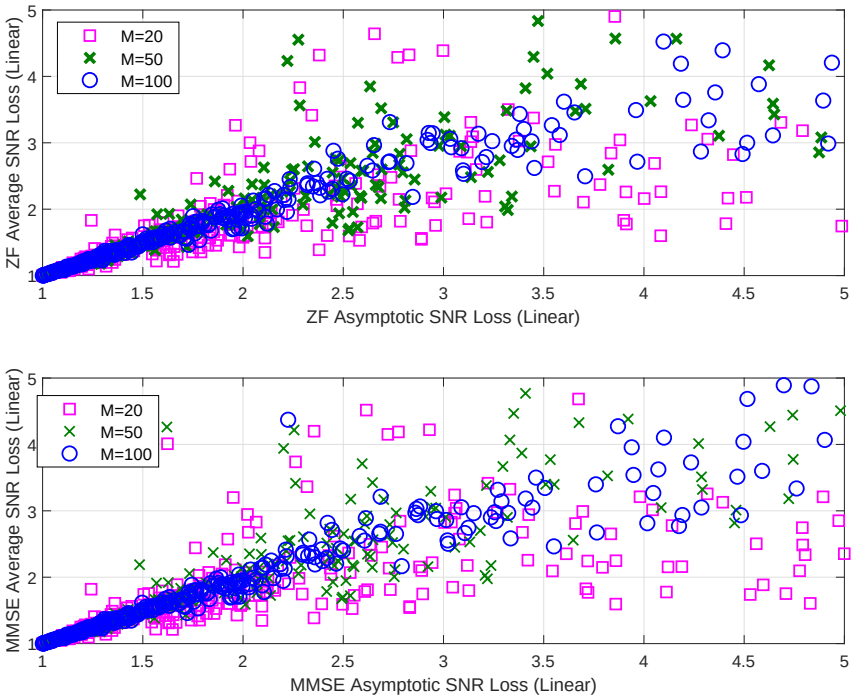

Figure 2: Asymptotic versus average SNR loss of ZF and MMSE cancelers for 1000 channel realizations for synthetic random channels $\mathbf{Q}$ of various sizes $M \in \{20, 50, 100\}$ with $0 \leq \sigma^2 < 1$ and single wire SNR $\eta = 30$ dB. The non-diagonal elements of $\mathbf{Q}$ are i.i.d and log-normally distributed generated with variance randomly chosen from the set $\sigma_{dB} = \{0, 5, 10\}$ dB and the corresponding mean is selected using $\mu_{dB} = 2.33\sigma_{dB}$ [38].

5.1. Synthetic Wireline Channels

We start with a simplified scenario by generating synthetic random channel matrices $\mathbf{Q}$ that satisfy the assumption AS1. Here, the diagonal elements of matrix $\mathbf{Q}$ are zero, while the non-diagonal elements are i.i.d and log-normally distributed with a mean and variance selected from [38]. In these simulations we used the zero, low and high coupling models of [38] to simu-

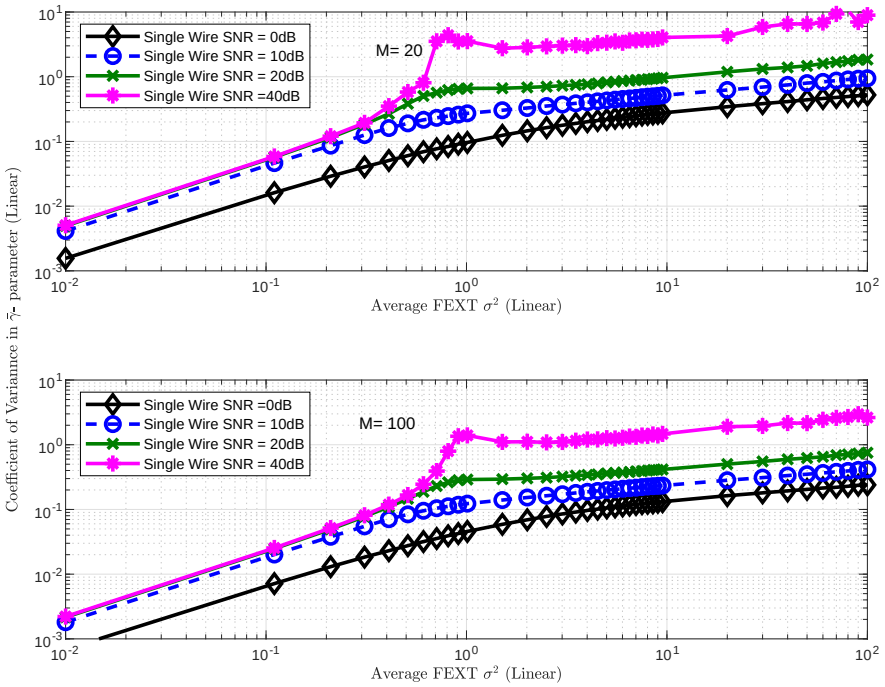

Figure 3: Coefficient of variation of the γ-parameter of the MMSE canceler for synthetic channel matrix $\mathbf{Q}$ of size $M = 20$ and $M = 100$ at various single wire SNRs, $\sigma_{dB} = 5$.

late a variety of wireline channels. The synthetic wireline channels provide a means to analyze the asymptotic performance for any value of σ^2 and single-wire SNR since the practical DSL channels have a limited range of these parameters, as discussed in the next subsection.

First, we consider $0 \leq \sigma^2 < 1$, single-wire SNR $\eta = 30$dB, and channel matrices of different sizes $M \in \{20, 50, 100\}$ to demonstrate the accuracy of the suggested approximation in (47) and (51). The metric of evaluation is the SNR loss which is defined as the reduction in the SNR with respect to the single-wire SNR. We compare the SNR loss computed by the empirical

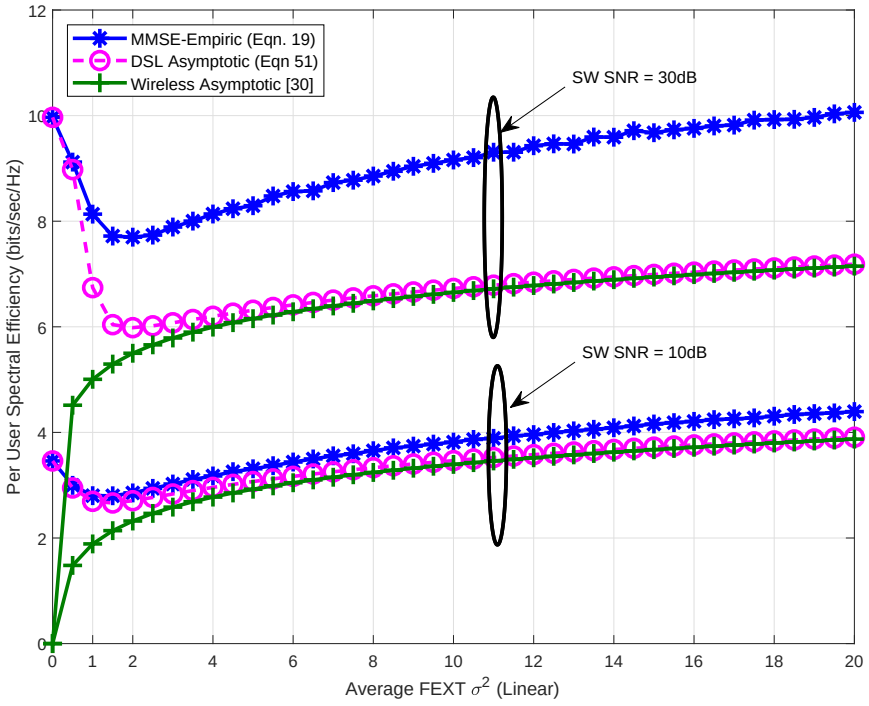

Figure 4: Performance of the DSL asymptotic analysis compared to the wireless asymptotic for the MMSE canceler for a synthetic random channel matrix $\mathbf{Q}$ of size $M = 20$, $\sigma_{dB} = 5$ dB.

average (i.e., average of 1000 channel realizations) and derived asymptotic expressions as shown in Fig. 2. The asymptotic SNR loss is computed using the positive root of (32) by considering $\zeta \to \infty$ and $\zeta = \eta$ for the ZF and the MMSE, respectively. Fig. 2 demonstrates the accuracy of asymptotic analysis for both ZF and MMSE cancelers. As can be seen, the asymptotic expressions yields an excellent accuracy as long as the average SNR loss is below 2 for moderate matrix ($M = 50$) and large matrix size ($M = 100$). It can also been seen that even for the small matrix size ($M = 20$), the

asymptotic expressions yields a good accuracy as long as the average SNR loss is below 2. Considering for example ZF and inspecting (42), $\gamma^o \leq 2$ implies $\sigma^2 \leq 1/2$. Thus, for the ZF, the approximation will be good as long as the total FEXT power is less than half of the power of the direct channel which is typically observed for DSL channels, as demonstrated in the next subsection.

Next, we consider $\sigma^2 > 1$ and different single-wire SNR values to study the accuracy of approximation for linear cancelers using the asymptotic analysis of the MMSE canceler, as depicted in Fig. 3. Here, the ZF asymptotic analysis is not useful since it approaches zero when $\sigma^2 > 1$ (as proved in Corollary 2). Since the ZF and MMSE are equivalent at high SNR, the MMSE asymptotic result can be used to approximate the ZF performance when $\sigma^2 > 1$. The metric for performance evaluation is the coefficient of variation (a statistical parameter) which is used here to demonstrate the accuracy of the approximation error. The coefficient of variation of the γ-parameter is defined as its standard deviation divided by the mean; i.e., $\frac{\sqrt{\mathbb{E}[|\bar{\gamma}-\gamma^{\circ}|^2]}}{\mathbb{E}[\bar{\gamma}]}$, where $\bar{\gamma}$ was given in (23). It is noted that a lower value of coefficient of variation denotes a higher accuracy. Fig. 3 demonstrates the coefficient of variation versus average FEXT for different values of single-wire SNR at a smaller ($M = 20$) and larger $M = 100$) matrix size. Comparing two subplots in Fig. 3, it can be easily seen that the accuracy of MMSE approximation is higher for a large matrix size. It can also be seen that the accuracy in the asymptotic approximation improves at a lower single-wire SNR but reduces as the average FEXT (σ^2) increases. However, the MMSE approximation still provides a reasonable accuracy in two scenarios: at a

lower SW-SNR and higher average FEXT, and at a lower average FEXT and higher SW-SNR. It is noted that these scenarios are typical for practical DSL channels and has been considered in the next subsection.

Finally, we conclude the performance evaluation for synthetic wireline channels by comparing the proposed asymptotic analysis of the MMSE to the asymptotic analysis developed for wireless channel [30], as depicted in Fig. 4. This will verify the correctness of the proposed analysis and demonstration of the claim in Theorem 3 that the wireless solution [30] is a special case of the generalized solution proposed in this paper. In contrast to the wireline channel whose diagonal elements (direct path for signal transmission) differ from the non-diagonal elements (crosstalk paths), the wireless analysis assumes that all the elements of channel matrix are identically distributed (due to random multi-paths[4]) [30]. Here, Fig. 4 compares the asymptotic approximation of the average spectral efficiency using the technique of wireless system [30], the proposed analysis in this paper, and the simulation results, for various average FEXT (σ^2) and single wire SNR η. The figure shows that that the approximation using the proposed wireline asymptotic performs quite well for the whole range of σ^2 for lower values of SW-SNR (10 dB), but for higher SW-SNR (30 dB) it is accurate only up to $\sigma^2 < 0.5$. Note that these are typical values observed in DSL systems. On the other

[4]Even in line of sight scenarios, the wireline channel differs from the wireless channel since the wireless channel will have the same statistics for all antennas (each antenna will see a line of sight component and a fading component). In contrast, in wireline, the diagonal element has a specific characteristic, because it is the only element with a direct wire connection.

Table 1: Simulation Parameters for DSL Wireline Systems

Number of users	$M = 10$ to 100
Band plan (G.fast)	106 MHz and 212 MHz
Band plan (VDSL)	30 MHz
Tone spacing (VDSL)	$\Delta_f = 4.3125$ KHz
Tone spacing (G.fast)	$\Delta_f = 51.75$ KHz
Signal PSD $f \leq 30$ MHz	-65 dBm/Hz
Signal PSD $30 < f \leq 106$ MHz	-76 dBm/Hz
Signal PSD $f > 106$ MHz	-79 dBm/Hz
Additive noise	-140 dBm/Hz
Noise margin	6 dB
Coding gain	5 dB
Target BER	10^{-7}
Shannon Gap Γ	9.75 dB
bit cap (VDSL)	15 bits
bit cap (G.fast)	12 bits

hand, the wireless asymptotic completely fails to predict the output SNR at low σ^2, where the effect of the diagonal elements is dominant (the wireless asymptotic actually converges to zero for $\sigma^2 \to 0$). Both approximations show similar behavior at higher FEXT (σ^2), where the effect of diagonal elements becomes negligible compared to the non-diagonal elements.

5.2. DSL Channel Models

After performance evaluation of asymptotic analysis over synthetic wireline channels in the previous subsection, we now consider more practical

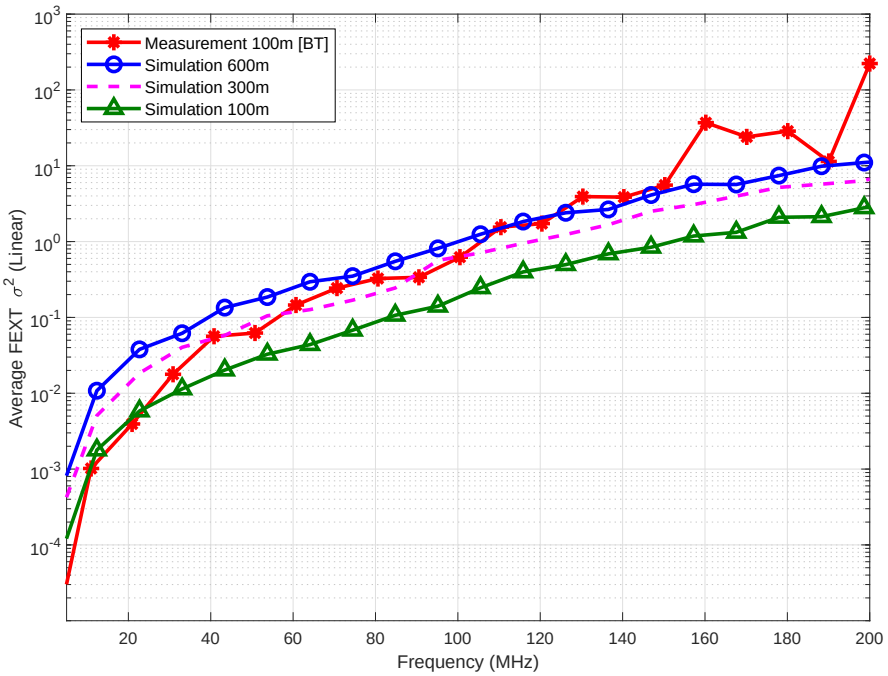

Figure 5: Average FEXT i. e., σ^2 of DSL measurement channel matrix [49] and simulated channel matrix (cable CAD55) of size $M = 10$ for G.fast frequencies.

scenarios of DSL systems to test the accuracy of the approximation. We consider both measured and simulated models of DSL channels from VDSL and G.fast systems. The measured channels for VDSL contained data from a 26 AWG cables with 28 pairs of various line lengths [34], while the measured channels for G.fast consist a 0.5 mm BT cable with 10 pairs each measuring 100 m [49]. The simulated channels were obtained using parametric DSL models (CAD55 cable) at various line lengths and binder size from ITU-T standards [3] [38]. The other parameters used in the simulations are listed in Table 1.

First, we present the average FEXT values of few DSL channels in Fig. 5 since the average FEXT is an important parameter used in the accuracy of asymptotic approximation. The figure shows that the average FEXT increases with frequency (since both crosstalk and attenuation increases with frequency) and can be very high ($\sigma^2 > 100$) at very high frequencies. At such high frequencies, there can be an issue of convergence of the asymptotic analysis, as demonstrated in Fig. 3. However, the SW-SNR becomes quite low which helps in the convergence of asymptotic approximation. Even with a mild approximation error, the impact on the overall data rate is indistinguishable since spectral efficiency at these higher tones is quite low, as shown in Fig. 6 and Fig. 7 for VDSL and G.fast channels, respectively. It is noted that the random behavior of the FEXT and the statistical characterization of the channel were studied using measured data in the conference version of this paper [1][5]. This also validated the requisite assumption AS1 from the measured DSL channels.

Next, we analyze the asymptotic approximation by evaluating the spectral efficiency performance of the ZF and MMSE cancelers over measured channels (for both VDSL and G.fast frequencies), as shown in Figures 6 and 7. The plots show the spectral efficiency per user (calculated by averaging (11) for the ZF and (19) for the MMSE) and the asymptotic approximation for the ZF canceler R^{ZF} in (47) and R^{MMSE} in (51) for the MMSE. As described earlier, we incorporate the Shannon-gap formalization $R_{\mathrm{mod}}(\mathrm{SINR}) = \log_2(1 + \mathrm{SINR}/\Gamma)$ which reduces the optimal throughput by

[5]The DSL channel is considered typically stationary; however, the FEXT coefficients are random which increases with frequencies.

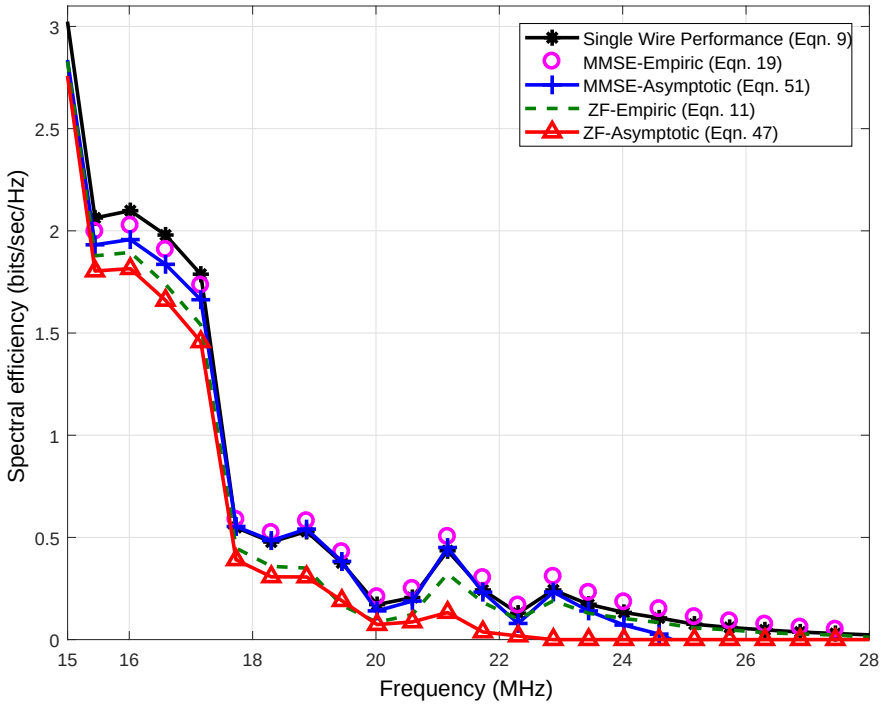

Figure 6: Performance of asymptotic analysis (spectral efficiency vs. frequency of transmission) of measurement channels for VDSL frequencies with $M = 28$, loop length of 590m, and cable type 26 AWG.

$\Gamma = 9.75$ dB for signal transmissions from a finite-QAM constellation. It is noted that DSL systems have constellation size in the range of 2 to 2^{15} QAM. For reference, we also depict the spectral efficiency of a single wire (setting $\mathbf{H} = \mathbf{I}$) such that only a single wire is active in a binder without the effect of crosstalk. Both figures show that the approximation is quite accurate for both the ZF and the MMSE cancelers for VDSL channels, even for longer loops (σ^2 increases with loop length). This takes place because of the smaller average FEXT, σ^2, as shown in Fig. 5. On the one hand, Fig. 7 shows that

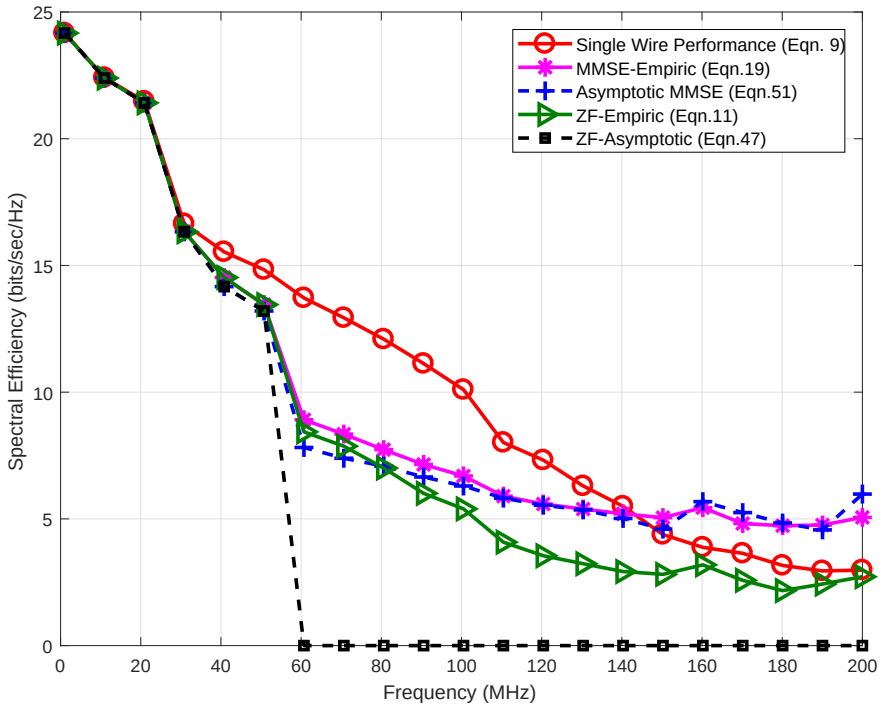

Figure 7: Performance of asymptotic analysis (spectral efficiency vs. frequency of transmission) of measurement channels for G.fast frequencies. The 100 user channel matrix is constructed by concatenating a randomly permuted version of the measured matrix of 10 pair data in [49].

the MMSE asymptotic result is quite accurate but the ZF asymptotic goes to zero above 60MHz. Note that the zero asymptotic result shows that the performance will deteriorate as the system size increases. Nevertheless, a zero is never a good approximation; hence, the ZF result is not useful for $\sigma^2 \geq 1$. Nevertheless, at these SNRs, the ZF performs quite close to the MMSE, and the MMSE asymptotic result gives quite a good approximation for both.

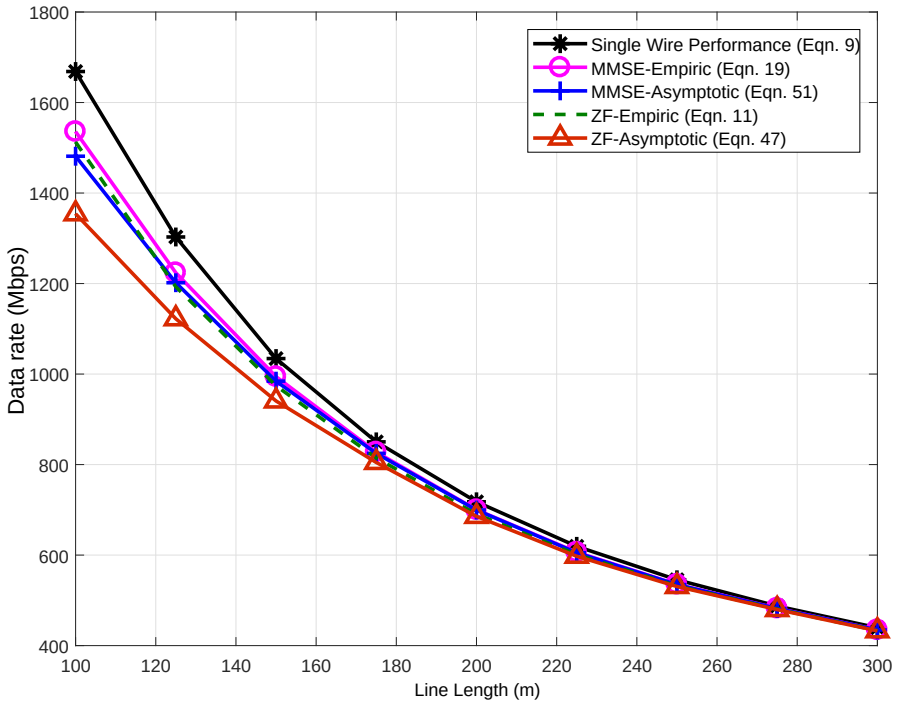

Figure 8: Average user rate performance of the asymptotic analysis (rate versus reach) using parametric DSL channels (CAD55) for G.fast 212 MHz. The binder is composed of 20 users with equal line lengths.

Finally, we evaluate the asymptotic performance of the ZF and MMSE cancelers in rate versus reach curves for parametric CAD55 DSL channel, as shown in Fig. 8. The rate-reach curves compared average data rates at a specific line length range for various channel realizations with that of the asymptotic approximation. Again, we incorporate the Shannon-gap formalization $R_{\text{mod}}(\text{SINR}) = \log_2(1 + \text{SINR}/\Gamma)$ for our numerical analysis. We obtain the aggregate data rates rates by summation of spectral efficiency of the ZF canceler in (11) and (47), and (19) and (51) for the MMSE perfor-

mance, over all DMT tones. Fig. 8 depicts the accuracy of approximation over 212 MHz G.fast systems. The figure shows that the approximation is quite accurate even for the G.fast system. However, the MMSE asymptotic is more accurate in predicting the performance of both the MMSE and the ZF cancelers. Since DSL systems operate at a very high SNR, the asymptotic analysis of the MMSE can also be used for ZF performance.

As seen from the above simulation results, the convergence of the proposed asymptotic analysis depends on many factors such as SW-SNR, average FEXT σ^2, and the matrix size M. If both the SW-SNR and average FEXT σ^2 are low, the convergence can be achieved even for matrix size of 10. However, with a higher values of average FEXT, the convergence might require larger matrix size. The above simulation results show that the convergence is achieved for a matrix size $M = 20$ for practical G.fast channels.

6. Conclusion

In this work, we presented an asymptotic analysis of the performance of ZF and MMSE receivers in a large matrix wireline system. We derived an approximation for the user rate for both the ZF and MMSE cancelers which are very simple to evaluate and does not need to take specific channel realizations into account. The analysis was based on the theory of large dimensional random matrices, but computer simulations over measured and simulated DSL channels showed that this approximation was accurate even for relatively low dimensional systems. We showed that the proposed asymptotic analysis converges excellently for relatively low FEXT or low SNR, and is thus useful for most scenarios in practical DSL systems.

Appendix A. Proof of Theorem 2

Substituting $\mathbf{\Psi}(-\frac{1}{\xi})$ and $\tilde{\mathbf{\Psi}}(-\frac{1}{\xi})$ from (28), the diagonal matrix $\mathbf{T}(-\frac{1}{\xi})$ can be represented as

$$\mathbf{T}(-\frac{1}{\xi}) = \text{diag}\Big(\frac{1}{\psi_1^{-1}(-\frac{1}{\xi}) + \frac{1}{\xi}\tilde{\psi}_1(z)}, \ldots, \frac{1}{\psi_n^{-1}(-\frac{1}{\xi}) + \frac{1}{\xi}\tilde{\psi}_n(-\frac{1}{\xi})}\Big). \tag{A.1}$$

Hence, the trace of $\mathbf{T}(-\frac{1}{\xi})$:

$$\text{tr}[\mathbf{T}(-\frac{1}{\xi})] = \sum_{k=1}^{n} \frac{1}{\psi_k^{-1}(-\frac{1}{\xi}) + \frac{1}{\xi}\tilde{\psi}_k(-\frac{1}{\xi})}. \tag{A.2}$$

Now, we substitute ψ_k and $\tilde{\psi}_k$ from (29) in (A.2) to get:

$$\text{tr}[\mathbf{T}(-\frac{1}{\xi})] = \sum_{k=1}^{n} \frac{1}{\frac{1}{\xi}\left(1 + \text{tr}\big(\tilde{\mathbf{\Omega}}_k\tilde{\mathbf{T}}(-\frac{1}{\xi})\big)/n\right) + \frac{1}{1+\text{tr}\big(\mathbf{\Omega}_k\mathbf{T}(-\frac{1}{\xi})\big)/n}}. \tag{A.3}$$

First, we prove the upper bound. Since $\xi \to \infty$ and $\text{tr}\big(\tilde{\mathbf{\Omega}}_k\tilde{\mathbf{T}}(-\frac{1}{\xi})\big)/n \geq 0$, (A.3) yields an upper bound on $\text{tr}[\mathbf{T}(-\frac{1}{\xi})]$ as

$$\begin{aligned} \text{tr}[\mathbf{T}(-\frac{1}{\xi})] &\leq \sum_{k=1}^{n} 1 + \sum_{k=1}^{n} \frac{1}{n}\text{tr}\left(\mathbf{\Omega}_k\mathbf{T}(-\frac{1}{\xi})\right) \\ &\leq n + \text{tr}\left(\frac{1}{n}\sum_{k=1}^{n}\mathbf{\Omega}_k\mathbf{T}(-\frac{1}{\xi})\right), \end{aligned} \tag{A.4}$$

where we used the identity $\text{tr}(\mathbf{A}+\mathbf{B}) = \text{tr}(\mathbf{A}) + \text{tr}(\mathbf{B})$ in the first term for $k = 1 \cdots n$. Using $\frac{1}{n}\sum_{k=1}^{n}\mathbf{\Omega}_k \leq \sigma_u\mathbf{I}$ from (30) and $t = \frac{1}{n}\text{tr}[\mathbf{T}(-\frac{1}{\xi})]$, (A.4) can be simplified to get $t \leq \frac{1}{1-\sigma_u^2}$. Similarly, we can analyze $\tilde{\mathbf{T}}(-\frac{1}{\xi})$ to prove that $\tilde{t} \leq \frac{1}{1-\sigma_u^2}$. Due to the uniqueness of the solution, and applying $\lim_{\xi\to\infty}$ to t or $\tilde{t}$, we get the upper bound in (39).

For the lower bound, we apply $\lim_{z\to 0^-}$ to (A.3):

$$\lim_{\xi\to\infty} \mathrm{tr}[\mathbf{T}(-\frac{1}{\xi})] = n + \mathrm{tr}\left(\frac{1}{n}\sum_{k=1}^{n} \mathbf{\Omega}_k \mathbf{T}(-\frac{1}{\xi})\right), \tag{A.5}$$

where we used the fact that $\tilde{\mathbf{\Omega}}_k \tilde{\mathbf{T}}(-\frac{1}{\xi})$ is bounded for every k. Using $\frac{1}{n}\sum_{k=1}^{n} \mathbf{D}_k \geq \sigma_l \mathbf{I}$ from (30) and $t = \frac{1}{n}\mathrm{tr}[\mathbf{T}(-\frac{1}{\xi})]$ in (A.5), we get $\gamma^\circ \geq \frac{1}{1-\sigma_l^2}$. Similarly, using $\tilde{\mathbf{T}}(-\frac{1}{\xi})$, we can have $\gamma^\circ \geq \frac{1}{1-\sigma_l^2}$, hence the lower bound in (39).

Acknowledgements

S. M. Zafaruddin was partially funded by the Israeli Planning and Budget Committee (PBC) post-doctoral fellowship.

References

[1] S. M. Zafaruddin, U. Klein, I. Bergel, A. Leshem, Asymptotic performance analysis of zero forcing DSL systems, in: 2016 IEEE International Conference on the Science of Electrical Engineering (ICSEE), 2016, pp. 1–5. doi:10.1109/ICSEE.2016.7806174.

[2] T. Starr, M. Sorbara, J. Cioffi, P. Silverman, DSL Advances, Prentice-Hall, Upper Saddle River, NJ, 2003.

[3] ITU-T G. 9701, ITU-T Recommendation G.9701-2014, Draft Recommendation ITU-T: Fast Access to Subscriber Terminals (FAST) :Physical layer specification G.9701, 2014.

[4] M. Timmers, M. Guenach, C. Nuzman, J. Maes, G.fast: evolving the copper access network, IEEE Communications Magazine 51 (2013) 74–79. doi:10.1109/MCOM.2013.6576342.

[5] S. M. Zafaruddin, I. Bergel, A. Leshem, Signal processing for gigabit-rate wireline communications: An overview of the state of the art and research challenges, IEEE Signal Processing Magazine 34 (2017) 141–164. doi:10.1109/MSP.2017.2712824.

[6] G. Ginis, J. M. Cioffi, Vectored transmission for digital subscriber line systems, Selected Areas in Communications, IEEE Journal on 20 (2002) 1085–1104.

[7] ITU-T G. 993.5, ITU-T Recommendation G.993.5: Self-FEXT Cancellation (Vectoring), 2010.

[8] R. Cendrillon, G. Ginis, E. Van den Bogaert, M. Moonen, A near-optimal linear crosstalk canceler for upstream VDSL, IEEE Transactions on Signal Processing 54 (2006) 3136–3146.

[9] R. Cendrillon, G. Ginis, E. Van den Bogaert, M. Moonen, A near-optimal linear crosstalk precoder for downstream VDSL, IEEE Transactions on Communications 55 (2007) 860–863. doi:10.1109/TCOMM.2007.896121.

[10] I. Wahibi, M. Ouzzif, J. L. Masson, S. Saoudi, Stationary interference cancellation in upstream coordinated DSL using a Turbo-MMSE receiver, International Journal of Digital Multimedia Broadcasting 2008 (2008).

[11] P. Pandey, M. Moonen, L. Deneire, MMSE-based partial crosstalk cancellation for upstream VDSL, in: IEEE International Conference on Communications (ICC), 2010.

[12] C.-Y. Chen, K. Seong, R. Zhang, J. M. Cioffi, Optimized resource allocation for upstream vectored DSL systems with zero-forcing generalized decision feedback equalizer, Selected Topics in Signal Processing, IEEE Journal of 1 (2007) 686–699.

[13] P. Tsiaflakis, J. Vangorp, J. Verlinden, M. Moonen, Multiple access channel optimal spectrum balancing for upstream DSL transmission, IEEE Communications Letters 11 (2007) 398–300. doi:10.1109/LCOM.2007.348280.

[14] S. Zafaruddin, S. Prakriya, S. Prasad, Performance analysis of zero forcing crosstalk canceler in vectored VDSL2, IEEE Signal Processing Letters 19 (2012) 219–222.

[15] I. Bergel, A. Leshem, The performance of zero forcing DSL systems, IEEE Signal Processing Letters 20 (2013) 527–530.

[16] A. Leshem, L. Youming, A low complexity linear precoding technique for next generation VDSL downstream transmission over copper, IEEE Transactions on Signal Processing 55 (2007) 5527–5534.

[17] I. Bergel, A. Leshem, Convergence analysis of downstream VDSL adaptive multichannel partial FEXT cancellation, IEEE Transactions on Communications 58 (2010) 3021–3027.

[18] I. Binyamini, I. Bergel, Adaptive precoder using sign error feedback for FEXT cancellation in multichannel downstream VDSL, IEEE Transactions on Signal Processing 61 (2013) 2383–2393.

[19] R. Strobel, M. Joham, W. Utschick, Achievable rates with implementation limitations for G.fast-based hybrid copper/fiber networks, in: 2015 IEEE International Conference on Communications (ICC), 2015, pp. 958–963. doi:10.1109/ICC.2015.7248446.

[20] R. Strobel, A. Barthelme, W. Utschick, Zero-forcing and MMSE precoding for G.fast, in: 2015 IEEE Global Communications Conference (GLOBECOM), 2015, pp. 1–6. doi:10.1109/GLOCOM.2015.7417707.

[21] A. Barthelme, R. Strobel, M. Joham, W. Utschick, Weighted MMSE Tomlinson-Harashima precoding for G.fast, in: 2016 IEEE Global Communications Conference (GLOBECOM), 2016, pp. 1–6. doi:10.1109/GLOCOM.2016.7842380.

[22] V. A. Marchenko, L. A. Pastur, Distribution of eigenvalues for some sets of random matrices, Matematicheskii Sbornik 114 (1967) 507–536.

[23] J. W. Silverstein, Z. Bai, On the empirical distribution of eigenvalues of a class of large dimensional random matrices, Journal of Multivariate analysis 54 (1995) 175–192.

[24] V. L. Girko, Theory of stochastic canonical equations, volume 2, Springer, 2001.

[25] A. M. Khorunzhy, B. A. Khoruzhenko, L. A. Pastur, Asymptotic properties of large random matrices with independent entries, Journal of Mathematical Physics 37 (1996) 5033–5060.

[26] R. B. Dozier, J. W. Silverstein, On the empirical distribution of eigenvalues of large dimensional information-plus-noise-type matrices, Journal of Multivariate Analysis 98 (2007) 678–694.

[27] W. Hachem, P. Loubaton, J. Najim, et al., Deterministic equivalents for certain functionals of large random matrices, The Annals of Applied Probability 17 (2007) 875–930.

[28] D. N. Tse, S. V. Hanly, Linear multiuser receivers: effective interference, effective bandwidth and user capacity, IEEE Transactions on Information Theory 45 (1999) 641–657. doi:10.1109/18.749008.

[29] D. N. Tse, O. Zeitouni, Linear multiuser receivers in random environments, IEEE Transactions on Information Theory 46 (2000) 171–188. doi:10.1109/18.817516.

[30] Y. C. Liang, G. Pan, Z. D. Bai, Asymptotic performance of MMSE receivers for large systems using random matrix theory, IEEE Transactions on Information Theory 53 (2007) 4173–4190. doi:10.1109/TIT.2007.907497.

[31] K. R. Kumar, G. Caire, A. L. Moustakas, Asymptotic performance of linear receivers in MIMO fading channels, IEEE Transactions on Information Theory 55 (2009) 4398–4418. doi:10.1109/TIT.2009.2027493.

[32] J. Hoydis, M. Kobayashi, M. Debbah, Asymptotic performance of linear receivers in network MIMO, in: 2010 Conference Record of the Forty Fourth Asilomar Conference on Signals, Systems and Computers, 2010, pp. 942–948. doi:10.1109/ACSSC.2010.5757706.

[33] S. Lin, Statistical behaviour of multipair crosstalk with dominant components, Bell Systems Technical Journal 59 (1980).

[34] N. Sidiropoulos, E. Karipidis, A. Leshema, L. Youming, Statistical characterization and modelling of the copper physical channel, Deliverable D2.1, EUFP6 STREP project U-BROAD #506790 (2004).

[35] J. Maes, M. Guenach, M. Peeters, Statistical MIMO channel model for gain quantification of DSL crosstalk mitigation techniques, in: 2009 International Conference on Communications (ICC), Dresden, Germany, June, 2009.

[36] R. van den Brink, Modeling the dual-slope behavior of in-quad EL-FEXT in twisted pair quad cables, IEEE Transactions on Communications PP (2017) 1–1. doi:10.1109/TCOMM.2017.2669032.

[37] E. Karipidis, N. Sidiropoulos, A. Leshem, L. Youming, R. Tarafi, M. Ouzzif, Crosstalk models for short VDSL2 lines from measured 30MHz data, EURASIP Journal on Applied Signal Processing 2006 (2006) 90–90.

[38] M. Sorbara, P. Duvaut, F. Shmulyian, S. Singh, A. Mahadevan, Construction of a DSL-MIMO channel model for evaluation of FEXT cancellation systems in VDSL2, in: Proc. of the IEEE Sarnoff Symposium, IEEE, 2007, pp. 1–6.

[39] M. Baldi, F. Chiaraluce, R. Garello, M. Polano, M. Valentini, Simple statistical analysis of the impact of some nonidealities in downstream

VDSL with linear precoding, EURASIP Journal on Advances in Signal Processing 2010 (2010) 90.

[40] A. Gomaa, N. Al-Dhahir, A new design framework for sparse FIR MIMO equalizers, IEEE Transactions on Communications 59 (2011) 2132–2140.

[41] J. M. Cioffi, A Multicarrier Primer, ANSI T1E1.4/91-157 (1991).

[42] C.-N. Chuah, D. N. Tse, J. M. Kahn, R. Valenzuela, et al., Capacity scaling in MIMO wireless systems under correlated fading, IEEE Transactions on Information Theory 48 (2002) 637–650.

[43] L. S. Cardoso, M. Debbah, P. Bianchi, J. Najim, Cooperative spectrum sensing using random matrix theory, in: 3rd International Symposium on Wireless Pervasive Computing, ISWPC, 2008, pp. 334–338.

[44] T. L. Marzetta, Noncooperative cellular wireless with unlimited numbers of base station antennas, IEEE Transactions on Wireless Communications 9 (2010) 3590–3600.

[45] L. Zheng, D. N. Tse, Diversity and multiplexing: a fundamental tradeoff in multiple-antenna channels, IEEE Transactions on Information Theory 49 (2003) 1073–1096.

[46] S. A. Jafar, S. Shamai, Degrees of freedom region of the MIMO channel, IEEE Transactions on Information Theory 54 (2008) 151–170.

[47] B. C. Jung, D. Park, W.-Y. Shin, Opportunistic interference mitigation achieves optimal degrees-of-freedom in wireless multi-cell uplink networks, IEEE Transactions on Communications 60 (2012) 1935–1944.

[48] ITU-T G. 993.1, Very high speed Digital Subscriber Line, ITU-T Recommendation G.993.1, Series G: Transmission Systems and Media, Digital Systems and Networks. (2004).

[49] L. Humphrey, G.fast: Release of BT cable measurements for use in simulations, ITU-T-SG15 contribution 2013-01-Q4-066 to G.fast (2013).

S.M. Zafaruddin (smzafar@biu.ac.il) received his Ph.D. degree in electrical engineering from the Indian Institute of Technology Delhi in 2013. His Ph.D. degree research was on crosstalk cancellation for vectored digital subscriber line (DSL) systems. From 2012 to 2015, he was with Ikanos Communications, Bangalore, India, working directly with the CTO Office, Red Bank, New Jersey, where he was involved in research and development for xDSL systems. Since 2015, he has been with the faculty of engineering at Bar-Han University, Ramat Gan, Israel, as a post-doctoral researcher working on signal processing for wireline and wireless communications. His current research interests include signal processing for communications, fifth-generation cellular networks, resource-limited sensor networks, and xDSL systems.

Itsik Bergel (itsik.bergel@biu.ac.il) received his B.Sc. degree (magna cum laude) in electrical engineering and his B.Sc. degree (magna cum laude) in physics from Ben Gurion University, Beersheba, Israel, in 1993 and 1994, respectively, and his M.Sc. degree (summa cum laude) and his Ph.D. degree in electrical engineering from the University of Tel Aviv, Israel, in 2000 and 2005, respectively. In 2005, he was a postdoctoral researcher at Politecnico

di Torino, Italy. He is currently a faculty member in the Faculty of Engineering, Bar-Ilan University, Ramat-Gan, Israel. His main research interests include multichannel interference mitigation in wireline and wireless communications, cooperative transmission in cellular networks, and cross-layer optimization of random ad hoc networks. Since 2015, he has served as an associate editor of IEEE Transactions on Signal Processing.

Amir Leshem (leshema@biu.ac.il) received his B.Sc. degree (cum laude) in mathematics and physics, his M.Sc. degree (cum laude) in mathematics, and his Ph.D. degree in mathematics from the Hebrew University, Jerusalem, Israel, in 1986, 1990, and 1998, respectively. In 2002, he joined Bar-Han University, Ramat-Gan, Israel, where he was one of the founders of the Faculty of Engineering and where he is a full professor and head of the communications research track. His main research interests include multichannel wireless and wireline communication, and applications of game theory to dynamic and adaptive spectrum management of communication networks. He was the leading guest editor for special issues on signal processing for astronomy and cosmology in IEEE Signal Processing Magazine and IEEE Journal of Selected Topics in Signal Processing.